

Disparities in particulate matter (PM₁₀) origins and oxidative potential at a city-scale (Grenoble, France) - Part II: Sources of PM₁₀ oxidative potential using multiple linear regression analysis and the predictive applicability of multilayer perceptron neural network analysis

Lucille Joanna S. Borlaza^{*1}, Samuël Weber¹, Jean-Luc Jaffrezo¹, Stephan Houdier¹, Rémy Slama², Camille Rieux³, Alexandre Albinet⁴, Steve Micallef³, Cécile Trébuchon³, and Gaëlle Uzu^{*1}

¹University of Grenoble Alpes, CNRS, IRD, INP-G, IGE (UMR 5001), F-38000 Grenoble, France

²University of Grenoble Alpes, Inserm, CNRS, IAB (Institute of Advanced Biosciences), Team of Environmental Epidemiology applied to Reproduction and Respiratory Health, Grenoble, France

³Atmo AuRA, F-38400 Grenoble, France

⁴INERIS, Parc Technologique Alata, BP 2, 60550 Verneuil-en-Halatte, France

Correspondence to: LJS Borlaza (lucille-joanna.borlaza@univ-grenoble-alpes.fr) and G Uzu (gaelle.uzu@ird.fr)

Abstract. The oxidative potential (OP) of particulate matter (PM) measures PM capability to potentially cause anti-oxidant imbalance. Due to the wide range and complex mixture of species in particulates, little is known on the pollution sources most strongly contributing to OP. A one-year sampling of PM₁₀ (particles with an aerodynamic diameter below 10) was performed over different sites in a medium-sized city (Grenoble, France). An enhanced fine-scale apportionment of PM₁₀ sources, based on the chemical composition, was performed using Positive Matrix Factorization (PMF) method and reported in a companion paper (Borlaza et al., 2020). OP was assessed as the ability of PM₁₀ to generate reactive oxygen species (ROS) using three different acellular assays: Dithiothreitol (DTT), Ascorbic acid (AA), and 2,7-dichlorofluorescein (DCFH) assays. Using multiple linear regression (MLR), the OP contribution of the sources identified by PMF were estimated. Conversely, since atmospheric processes are usually non-linear in nature, artificial neural network (ANN) techniques, which employs non-linear models, could further improve estimates. Hence, the multilayer perceptron analysis (MLP), an ANN-based model, was additionally used to model OP based on PMF-resolved sources as well. This study presents the spatiotemporal variabilities of OP activity with influences by season-specific sources, site typology and specific local features, and assay sensitivity. Overall, both MLR and MLP effectively captured the evolution of OP. The primary traffic and biomass burning sources were the strongest drivers of OP in the Grenoble basin. There is also a clear redistribution of source-specific impacts when using OP instead of mass concentration, underlining the importance of PM redox activity for the identification of potential sources of PM toxicity. Finally, the MLP generally offered improvements in OP prediction especially for sites where synergistic and/or antagonistic effects between sources are prominent, supporting the value of using ANN-based models to account for the non-linear dynamics behind the atmospheric processes affecting OP of PM₁₀.

1 Introduction

One of the most critical pollutants in the atmosphere is particulate matter (PM), especially in urban areas that are heavily impacted by anthropogenic emissions (David et al., 2019; Qiao et al., 2018; Schwela, 2000). Recent studies showed increasing interest in PM at a city-level allowing assessment of fine-scale pollution variability (Boppana et al., 2019; Dionisio et al., 2010; Etyemezian et al., 2005; Krasnov et al., 2016; Padhi and Padhy, 2008). The intricate topography and seasonality of particulate air pollution in the city of Grenoble (France) makes it an ideal location to explore variabilities of PM pollution, while also accounting for different site typologies within a single medium-sized city (Calas et al., 2019a; Favez et al., 2010; Srivastava et al., 2018; Tomaz et al., 2016, 2017; Weber et al., 2019). Such small-scale variabilities for mass and chemical composition have been recently addressed in a companion paper (Borlaza et al., 2020).

Many research studies have focused on the links between PM mass exposure and various adverse health effects (Dabass et al., 2018; Delfino et al., 2005; Du et al., 2016; Hime et al., 2018; Lao et al., 2019; Matus C. and Oyarzún G., 2019; Pope et al., 2009; Pope III, 2002; Winterbottom et al., 2018). However, it is also of high concern to improve the understanding of the PM sources in relation with such health impacts. Indeed, oxidative stress is now well recognized as one of the main biological mechanisms considered to be contributing to these detrimental impacts from air pollution exposure through the capability of PM to generate reactive oxygen species (ROS) within the lung, which leads to pro-inflammatory responses that can ultimately result in apoptosis (Ayres et al., 2008; Baulig et al., 2003; Dhalla et al., 2000; Donaldson et al., 2001; Jin et al., 2018; Kelly, 2003; Leni et al., 2020; Mudway et al., 2020; Nel, 2005; Piao et al., 2018). The oxidative potential (OP) of PM, defined as the capability of PM to generate ROS/[deplete anti-oxidants](#), makes an interesting complementary to regulated metrics of ambient PM exposure (Bates et al., 2019; Daellenbach et al., 2020; Guo et al., 2020; Gurgueira et al., 2002; Park et al., 2018; Shiraiwa et al., 2017; Valavanidis et al., 2008).

Most studies often correlate OP from PM with chemical species in ambient aerosols (Bell and HEI Health Review Committee, 2012; Boogaard et al., 2012; Borlaza et al., 2018; Cassee et al., 2013; Janssen et al., 2014; Perrone et al., 2016; Pietrogrande et al., 2018; Rohr and Wyzga, 2012; Yang et al., 2015). However, due to the wide range and complex mixture of PM and the dynamic atmospheric processes to consider, the main drivers of OP can be difficult to highlight (Calas et al., 2019a). Several methods have been used to assign the sources of OP, including the application of receptor modelling techniques such as Positive Matrix Factorization (PMF) and Chemical Mass Balance (CMB) (Ayres et al., 2008; Bates et al., 2015; Cesari et al., 2019; Fang et al., 2016; Paraskevopoulou et al., 2019; Verma et al., 2014; Weber et al., 2018, 2021; Yu et al., 2019; Zhou et al., 2019), Principal Component Analysis (PCA) (Borlaza et al., 2018; Conte et al., 2017), and Robotic Chemical Mass Balance (RCMB) coupled with Multiple Linear Regression (MLR) analysis (Argyropoulos et al., 2016). With these current techniques, the OP of PM has been linked to specific emission sources and their estimated contributions. However, a non-linear relationship of redox active components of PM is generally observed (Arangio et al., 2016; Calas et al., 2017; Charrier and Anastasio, 2015; Li et al., 2012; Xiong et al., 2017; Yu et al., 2018), hence traditional deterministic models could be, in some way, limited.

65 Approaches using artificial neural network (ANN) analysis have demonstrated enhanced results compared to classical models
when predicting PM from different variables such as meteorological data (Abderrahim et al., 2016; Chaloulakou et al., 2003;
Díaz-Robles et al., 2008; Hooyberghs et al., 2005; Huang and Kuo, 2018; McKendry, 2002; Papanastasiou et al., 2007; Perez
and Reyes, 2006), satellite-derived aerosol products (Gupta and Christopher, 2009), and other traffic-related variables
(Cabaneros et al., 2020, 2017; Gietl and Klemm, 2009; He et al., 2015). The ANN-based models, such as multilayer perceptron
70 (MLP), support pattern recognition and could extract trends from non-linear data, making it an interesting and competitive
innovative method of analysis in many scientific disciplines, including air quality studies (Cabaneros et al., 2019;
Chattopadhyay and Bandyopadhyay, 2007; Dorling et al., 2003; García Nieto et al., 2018; Gupta and Christopher, 2009; Jiang
et al., 2004; Ordieres et al., 2005; Perez and Reyes, 2006). Since atmospheric processes are generally non-linear in nature,
exploring the features of MLP could provide meaningful results closer to realistic estimates than most linear models
75 (Elangasinghe et al., 2014; Eldakhly et al., 2017; Gerken et al., 2006; Kukkonen, 2003; Nathan et al., 2017; Rahimi, 2017).
This study takes advantage of the enhanced source apportionment obtained in the companion paper (Borlaza et al., 2020),
revealing the fine-scale spatiotemporal characteristics of PM sources within a medium-size city area (Grenoble basin),
specifically in three different urban environments (background, hyper-center, and peri-urban typologies). Here, the main
drivers of OP are first attributed to PM sources (resolved by PMF) using a classical MLR analysis. Second, the possible
80 advantages of MLP analysis are also evaluated to compare MLP prediction of OP activity with MLR prediction. In summary,
by taking the opportunity of this unique database on PM chemistry and OP, we aim to investigate mainly on two innovative
questions:

1. Is there variability in the OP activity within a medium-sized urban area, and can this be related to the variability of the
contributions of the emissions sources?
- 85 2. Can MLP be used to accurately model the spatiotemporal evolution of OP by taking the PM source contributions as input
variables and if so, does it catch the non-linear pattern of OP?

2 Materials and methods

2.1 Site description and PM₁₀ sampling collection

The sampling sites and samples used in this study are described in detail in the companion paper (Borlaza et al., 2020). Briefly,
90 the sampling sites are located in the city of Grenoble in the southeast of France, as illustrated in Figure 1. The mountainous
environment in the area restricts atmospheric movements and promotes the development of atmospheric thermal inversions,
resulting in an increase of pollutant concentrations, especially during the winter season (Bessagnet et al., 2020; Tomaz et al.,
2017). The three measurement sites are located in an urban background (UB, Les Frênes), urban hyper-center (UH, Caserne
de Bonne), and peri-urban (PU, Vif), all within 15 km from the city center of Grenoble. The UB site is an established urban
95 background reference site for the regional air quality monitoring network (Atmo Auvergne Rhône-Alpes) in the south of the
city and largely investigated previously (Srivastava et al., 2018; Tomaz et al., 2016). The PU site is in a suburban area having

rural residential areas adjacent to an urbanization (low-density area), where biogenic emissions are prominently expected as the site is on the foot of the Vercors and Belledune mountain ranges. Lastly, the UH site is in the hyper-center of Grenoble and, despite being in a pedestrian area, is the most highly exposed to surrounding commercial and traffic emissions amongst the three sites.

The daily (24-h) filter-based PM₁₀ (particles ≤10 μm in diameter) sampling was performed with a 3-day interval for about one year (February 28, 2017 to March 10, 2018, sampling starts at 00:00 CEST) obtaining a total of about 130 samples per site. PM₁₀ was collected using a high volume sampler (Digitel DA-80, 30 m³ h⁻¹) onto 150 mm-diameter quartz fiber filters (Tissu-quartz PALL QAT-UP 2500 diameter 150 mm) following the recommendations of EN 12341:2014 procedures (CEN, 2014). All filters underwent a preheating treatment at 500°C for 12 hours to avoid any organic contamination. Additionally, field blank filters (n=20) were collected to determine the detection limits of the applied chemical analysis and to secure quality of samples during transport, setup, and recovery. The total PM₁₀ mass concentration was also simultaneously measured using tapered element oscillating microbalance equipped with filter dynamics measurement systems (TEOM-FDMS) (CEN, 2017; Grover, 2005).

110

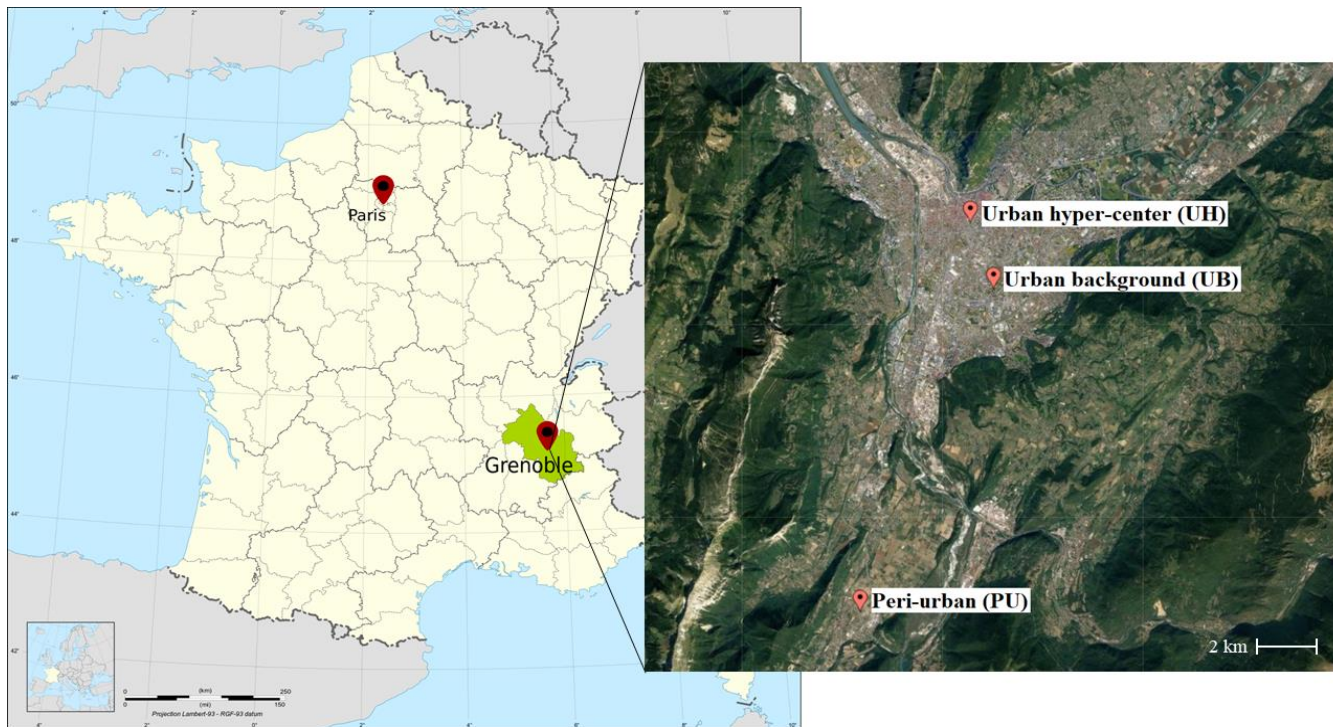


Figure 1: Study area in Grenoble (France) on a European map (left) and location of the three urban sites (right), namely Les Frênes or UB (urban reference background site), Caserne de Bonne or UH (urban hyper-center site), and Vif or PU (peri-urban site). ©OpenStreetMap contributors 2020. Distributed under a Creative Commons BY-SA License

115 2.2 Chemical characterization

All samples were subjected to several chemical analyses to quantify major and minor constituents of PM₁₀ including organic carbon (OC), elemental carbon (EC), ions (sodium (Na⁺), ammonium (NH₄⁺), potassium (K⁺), magnesium (Mg²⁺), calcium (Ca²⁺), chloride (Cl⁻), nitrate (NO₃⁻), sulfate (SO₄²⁻), methane sulfonic acid (MSA), organic acids (3-MBTCA, pinic acid, phthalic acid), anhydro-sugars (levoglucosan and mannosan) and primary saccharides (arabitol and mannitol, hereafter summed up and referred as polyols), cellulose, and elements (Al, As, Ba, Cd, Cr, Cu, Fe, Mn, Mo, Ni, Pb, Rb, Sb, Se, Sn, Ti, V, Zn). Detailed descriptions of the chemical analyses are available in the companion paper (Borlaza et al., 2020) and a summary of PM₁₀ characteristics is available in Table S1 the supplementary information (S1).

2.3 OP analysis

For OP analysis, the filters were subjected to PM₁₀ extraction using a simulated lung fluid (SLF) solution composed of a Gamble + DPPC (dipalmitoylphosphatidylcholine) mixture (Calas et al., 2018). In order to maintain a constant amount of extracted PM₁₀, filter punches were adjusted by area to obtain iso-mass at 25 µg ml⁻¹. No filtration was done in order to include both water soluble and insoluble particles. Such extraction method has been adopted to facilitate the extraction of PM₁₀ in conditions closer to lung physiology (Calas et al., 2017). To avoid the interferences in the wells by insoluble particles, we subtracted the intrinsic absorbance of all PM extractions before adding the reactants. This procedure has been tested on both soluble and insoluble compounds that are likely within the range of atmospheric concentrations. The results have confirmed good dispersion of particles, leading to homogeneous results. A more detailed report is available in Calas et al. (2018). For positive control tests, the 1,4-naphthoquinone (1,4-NQ) was used for both DTT and AA assays. Particularly, a 40 µl of 24.7 µM stock solution was used for DTT assay and an 80 µl of 24.7 µM 1,4-NQ solution for AA assay (Calas et al., 2017, 2018). A 100 nM H₂O₂ was used for DCFH assay. The measurement quality was estimated by calculating the coefficient of variation (CV) of the positive controls, all CVs were <3% for the 3 assays. Additionally, an ambient filter collected from the lab roof, with a known and constant expected OP value, was analysed to ensure precision of OP measurements.

The OP activity can be represented using two different measures: 1) the mass-normalized OP activity (OP_m), where OP is normalized by the mass of PM₁₀ (µg), and 2) the volume-normalized OP activity (OP_v), where OP is normalized by the sampled air volume (m³). The OP_m is the intrinsic OP property of one µg of PM, while OP_v represents the PM-derived OP per m⁻³ of air. Three a-cellular complementary assays were used to perform OP measurements and are briefly described in the following sections. All samples were subjected to triplicate analysis and each sample results in the mean of such triplicate. The common coefficient variation (%CV)CV is between 0 and 10% for each assay.

2.3.1 Dithiothreitol (DTT) assay

DTT is considered as a chemical surrogate to cellular reducing agents, nicotinamide adenine dinucleotide (NADH) and nicotinamide adenine dinucleotide phosphate-oxidase (NADPH), to mimic in vivo interactions of PM and biological oxidants.

The consumption of DTT in the assay is inferred as a measure of the ability of the PM to transfer electrons from DTT to oxygen thereby producing reactive oxygen species (ROS). Our procedure is based on a modified protocol by Cho et al. (2005), as described in Calas et al. (2018). The PM₁₀ extracts were reacted with DTT resulting to the consumption of DTT in the solution. The remaining DTT is then titrated with 5,5-dithiobis-(2-nitrobenzoic acid) (DTNB) to produce a yellow chromophore (5-mercapto-2-nitrobenzoic acid or TNB), which is in direct proportion to the amount of reduced DTT remaining in solution after the reaction with the PM₁₀ extract. These mixtures were injected in a 96-well plate (CELLSTAR, Greiner-Bio) and the consumption of DTT (nmol min⁻¹) was determined by following the TNB absorbance at 412 nm wavelength using a microplate-reader (TECAN spectrophotometer Infinite M200 Pro) at 10-minute intervals for a total of 30 minutes of analysis time.

2.3.2 Ascorbic acid (AA) assay

The AA assay is based on a modified procedure by (Kelly and Mudway, 2003), as described in Calas et al. (2018), using a respiratory tract lining fluid (RTFL). This assay uses AA, a known antioxidant which prevents the oxidation of lipids and proteins in the lung lining fluid (Valko et al., 2005). The consumption of AA (nmol min⁻¹) in the assay is inferred as the OP of PM₁₀ quantified by the transfer of electrons from AA to oxygen (O₂). Similar to the DTT assay, the PM₁₀ extracts were reacted with AA into a 96-well plate UV-transparent (CELLSTAR, Greiner-Bio). The absorbance was measured at 265 nm using a plate-reader (TECAN spectrophotometer Infinite M200 Pro) at 4-minute intervals for a total of 30 minutes of analysis time.

2.3.3 Dichloro-dihydro-fluorescein diacetate (DCFH) assay

The 2,7-dichlorofluorescein (DCFH) assay is commonly used for detecting intracellular H₂O₂ and oxidative stress using a non-fluorescent probe through the formation of a fluorescent product (dichlorofluorescein or DCF) in the presence of ROS and horseradish peroxidase (HRP). The DCF is measured by fluorescence at the excitation and emission wavelengths of 485 and 530 nm, respectively, every 2 minutes for a total of 30 minutes of analysis time. The ROS concentration in the sample is calculated in terms of H₂O₂ equivalent based on a H₂O₂ calibration (100, 200, 300, 400, 500, 1000, and 2000 nmol).

2.4 Data analysis

2.4.1 Synthesis of the methodology used for PM₁₀ source apportionment

The source apportionment performed on this dataset has been described into details in the companion paper (Borlaza et al., 2020). In brief, the PMF methodology used the EPA PMF5.0 software (US EPA, Norris et al. (2014)) and closely follows the parameterization used in previous works by our group (Favez et al., 2017; Waked et al., 2014; Weber et al., 2019, 2021) with a few relevant modifications.

The input variables used were mass concentration and uncertainty levels of PM₁₀ and its chemical composition (a total of 35 variables) including OC, EC, ions, elements, and some organic markers (MSA, levoglucosan, mannosan, polyols, pinic acid, 3-MBTCA, phthalic acid, and cellulose). The associated uncertainties were calculated based on a method proposed by Gianini

et al. (2012). Specific geochemical constraints, based on expert prior knowledge, were added to the solution using the ME-2 solver (Paatero, 1999), particularly for the traffic source factor (Charron et al., 2019). The statistical validity of the solution and the uncertainties were estimated using the bootstrap and displacement methods following the European recommendation for source apportionment studies (Belis et al., 2019; Brown et al., 2015). The specific tracers used to identify the sources are presented in Table S2 in the supplementary information (S2).

2.4.2 Multiple linear regression (MLR) analysis

A multiple linear regression (MLR) analysis was performed to attribute OP from the PMF-resolved sources of PM₁₀, following the OP deconvolution methodology proposed by Weber et al. (2018). The OP_v from the three assays were used individually as the dependent variable, while the PMF-resolved source contributions were used as independent variables, as shown in Eq.1:

$$OP_{obs} = (G_n \times \beta_n) + \varepsilon, \quad (1)$$

where OP_{obs} is the observed daily OP_v , matrix of size $d \times 1$ in $\text{nmol}_{\text{reactant}} \text{min}^{-1} \text{m}^{-3}$, G is the contribution of the sources from the PMF in $\mu\text{g} \text{m}^{-3}$ of size $d \times n$ and β is the regression coefficient representing the intrinsic OP (or the OP_m) of size $1 \times n$ in $\text{nmol} \text{min}^{-1} \mu\text{g}^{-1}$. Finally, ε is the residual term accounting for the difference between the observed and modeled OP of size $d \times 1$ in $\text{nmol}_{\text{reactant}} \text{min}^{-1} \text{m}^{-3}$. The OP contribution of each source is calculated by multiplying the source-specific regression coefficient by the contribution of the source to PM₁₀ ($G_k \times \beta_k$).

2.4.3 Multilayer perceptron (MLP) neural network analysis

2.4.3.1 Background of the MLP analysis

The MLP analysis is designed using a feed forward learning model (Calcagno et al., 2010; García Nieto et al., 2018; Salazar-Ruiz et al., 2008) that produces a predictive model for one or more output variables (OP_v) based on the values of the input variables (PM₁₀ source contributions). The three main components of MLP are: 1) the input layer, 2) the hidden layer, and 3) the output layer. Generally, the MLP consists of interconnected layers of artificial neurons that form a network using a set of input data and draws it onto a set of output data, which are then used to further train the neural network through a back-propagation process (Bishop, 1995; Fontes et al., 2014; Kim and Gilley, 2008). In this study, the neural network architecture was limited to a one hidden layer design to demonstrate the applicability of non-linear models, even only with a rudimentary architecture, and to compare its predictive capability against that of MLR.

2.4.3.2 Implementation of the MLP

As an initial step, a rescaling process is applied to both the input and output layers to eliminate potential bias due to the range of variance within the dataset (Gardner and Dorling, 1998). Each variable is standardized by subtracting the mean observed value and then divided by the standard deviation. The daily contributions of the PM sources obtained from the PMF were fed in the input layer to the hidden layer. The MLP analysis was performed for each site using the OP_v from each assay (OP_v^{DTT} ,

OP_v^{AA} , and OP_v^{DCFH}) as multiple variables in the output layer (see [Figure 2](#)), making a set of 9 independent studies. At each node (or neuron), the information given by the input neurons are condensed into a unique value and propagated to the next layer. For instance, the MLP described in [Figure 2](#) is formally defined by Eq. 2 for the first layer (hidden layer):

$$\forall_j \in \{1, \dots, l\}, z_j = H\left(\sum_{i=1}^d w_{i,j}^G \times x_i + w_{0,j}^G\right) \quad (2)$$

with $w_{i,j}^G$ the weight of the neuron between the input and hidden layer and $w_{0,j}^G$ an activation constant for neuron j. The activation function H is often non-linear.

To sum up, the hidden layer develops the input data and deciphers the relationship of the neurons within the MLP network. The number of neurons in the hidden layer was determined automatically by the estimation algorithm. With the activation function, the hidden layer transfers a response onto the output layer. The activation functions tested in this study were sigmoid and hyperbolic tangent (TanH) as these are appropriate for continuous dependent variables (IBM, 2016). A weight initialization was preset for potential occurrence of vanishing gradients (Bengio et al., 1994; Hochreiter, 1998; Hochreiter and Schmidhuber, 1997). The scaled conjugate and stochastic gradient descent optimization algorithms were tested to obtain the optimal weights in both the input and output layers (Slini et al., 2006; Vakili et al., 2015). The various MLP architectures tested are summarized in the supplementary information (S3).

220

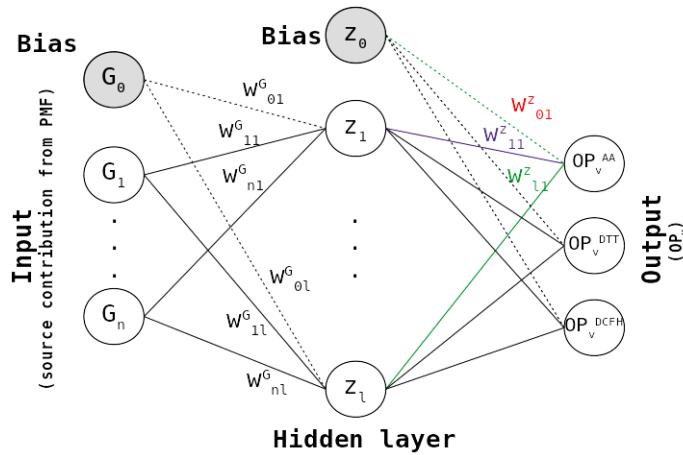


Figure 2: The MLP neural network architecture used in this study, where n refers to the number of source, G is the normalized contribution from the PMF, and OP_v is the different volume-normalized OP activities (OP_v^{DTT} , OP_v^{AA} , and OP_v^{DCFH})

The dataset was partitioned into: 1) the training set accounting for 80%, and 2) the testing set accounting for 20% of the dataset. For each of the 9 studies, the training set contains data points that were used to train the MLP, while the testing set is an independent set of data points used to monitor errors during the training step. During the training step, the MLP is continually developed and refined until the weighting values between the nodes accurately predict the outcome (i.e., minimal possible errors). To prevent the model from over-fitting, a set of stopping rules are applied to terminate the training of the MLP when any of these scenarios occur such as: 1) there is no decrease in prediction error for more than 1 step, 2) the maximum training

225

230 time is reached (15 minutes), 3) the minimum relative change in training error is reached (0.0001), 4) the minimum relative
change in training error ratio is reached (0.001). A maximum of 1000 data passes (epochs) are stored in memory until this step
is completed. Using the results obtained in the training step, the results are validated in the testing step to check the performance
of the network by assessing its forecasting capability on data points outside the training set. The MLP neural network analysis is
was performed using IBM SPSS Statistics for Windows, version 20 (IBM Corp., Armonk, N.Y., USA).

235 2.4.3.3 Demonstration of the non-linear behaviour of sources using the MLP models

Since MLP analysis should account for the interactions between PM₁₀ sources, the non-linear atmospheric dynamics causing
possible synergistic or antagonistic effects on the OP activity can be captured. To visualize such possible non-linear behaviour,
the MLP models obtained were applied on a set of dummy datasets. Each dummy dataset consists of the same mass
contributions (from PMF analysis) of each source (in µg m⁻³) as in the original dataset but setting one source (*n*) to zero.

240 This modelled OP using a dummy dataset (MLP_n) is subtracted to the modelled OP by the original MLP model (MLP)
(containing all source contributions). This difference represents a source-specific OP contribution and their summation
(MLP_{sum}) is described in Eq. 3:

$$MLP_{sum} = \sum MLP_n \quad (3)$$

For example, if the biomass burning source contributions was set to zero in the dummy dataset ($MLP_{n=biomass\ burning}$), then
245 ($MLP - MLP_{n=biomass\ burning}$) represents the MLP-modelled OP contribution of the biomass burning source. Assuming there
is completely no synergistic or antagonistic effects between PM₁₀ sources, then the original MLP-modelled OP contributions
should be equal to the sum of all source-specific OP contributions ($MLP = MLP_{sum}$). In cases where $MLP > MLP_{sum}$, then
synergistic effects are highlighted between some PM₁₀ sources resulting in an increased MLP-modelled OP activity.
Conversely, where $MLP < MLP_{sum}$ highlights antagonistic effects between some PM₁₀ sources resulting in a decreased MLP-
250 modelled OP activity.

2.4.4 Statistical analysis

For the comparison of temporal variations of the observed measurements, all the correlations were evaluated using Spearman
rank correlation coefficients (r_s), where $p \leq 0.05$ is considered statistically significant. For the comparison of OP measures, the
correlations were evaluated using Pearson correlation coefficients (r), where $p \leq 0.05$ is considered statistically significant. For
255 the evaluation and comparison of model performance between the MLR and MLP results, a number of performance indicators
were calculated such as the goodness-of-fit (R^2), root mean square error (RMSE), and Pearson correlation coefficient (r). The
STATA/SE version 15.1 software (College Station, TX, USA) or Python libraries was used for the statistical analyses.

3 Results and discussion

3.1 Temporal variation of PM₁₀ and OP activity

260 The daily distributions of PM₁₀ and OP activity (OP_v^{DTT} , OP_v^{AA} , and OP_v^{DCFH}) for each site are provided in the supplementary information (S4). [The range of the OP measurements in Grenoble are well within the range of measurements in France \(Calas et al., 2018, 2019b; Weber et al., 2021, 2018\)](#). Detailed discussion of the temporal variability of PM₁₀ sources is available in the companion paper (Borlaza et al., 2020).

Overall, the average PM₁₀ concentrations on days of measurements were higher during the colder months (October to April) at 17±10 µg m⁻³ and lower during the warmer months (May to September) at 10±4 µg m⁻³ in the city of Grenoble. With the alpine environment and the atmospheric dynamics in the study area, the occurrence of atmospheric inversions and the restriction of strong winds often results to higher concentration levels of air pollutants especially in the winter season (Bessagnet et al., 2020; Tomaz et al., 2017). Such observed seasonality in PM₁₀ mass concentration is also commonly explained by higher contributions from the biomass burning source in the colder seasons, especially in an alpine valley as previously reported in previous studies (Calas et al., 2019a; Favez et al., 2010; Herich et al., 2014; Srivastava et al., 2018; Tomaz et al., 2016, 2017; Weber et al., 2018, 2019). In the same way, a seasonality is displayed in OP activity in the Grenoble basin as well. In fact, the average daily OP activity levels during the winter season can be up to 2, 7, and 5 times higher than in summer season for OP_v^{DTT} , OP_v^{AA} , and OP_v^{DCFH} , respectively. Indeed, the observed strong seasonality (higher OP during winter, lower OP during summer) at all sites could induce a high spatial homogeneity between sites as well. However, there are a number of local features observed at different sites such as spikes in the OP activity during the warmer months at UH and PU sites (see Figure S1 in the supplementary information (S5)). These spikes are prominently seen in the OP_v^{DTT} , with also some occurrences in the OP_v^{AA} and OP_v^{DCFH} , which also emphasizes on the sensitivity of each assay.

Previous studies have reported that the OP_v^{DTT} has shown higher sensitivity with organics, metals, and the synergistic effect of the two (Bates et al., 2019; Dou et al., 2015; Fang et al., 2017; Gao et al., 2020b, a; Jiang et al., 2019; Weber et al., 2021; Yu et al., 2018), while OP_v^{AA} being sensitive mostly to metals concentrations (Bates et al., 2019; Crobeddu et al., 2017; Visentin et al., 2016; Weber et al., 2021). Table S4 in the supplementary information (S9) summarizes several publications on OP assays and their correlations to chemical species. In our study, a good correlation ($r=0.68$) was found between OP_v^{DTT} and OP_v^{AA} when all sites are combined (see Figure S1 in the supplementary information (S5)), possibly affected by the local features solely captured by the DTT assay. Due to the sensitivity to various ROS and RNS (reactive nitrogen species) of most molecular probes, the sensitivity of DCFH assay to specific components of PM₁₀ can be difficult to isolate (Bates et al., 2019; Jovanovic et al., 2019). However, OP_v^{DCFH} showed good correlation ($r=0.68$) with OP_v^{DTT} and an even stronger correlation ($r=0.93$) with OP_v^{AA} (see Figure S2 in the supplementary information (S5)).

The comparison of the two OP measures, OP_v and OP_m , of each OP assay can provide information regarding the dependency of OP activity to PM₁₀ mass concentration. As shown in Figure S3 in the supplementary information (S5), there is only a moderate correlation ($r=0.51$) between OP_v^{DTT} and OP_m^{DTT} suggesting the dependency of DTT assay to chemical composition

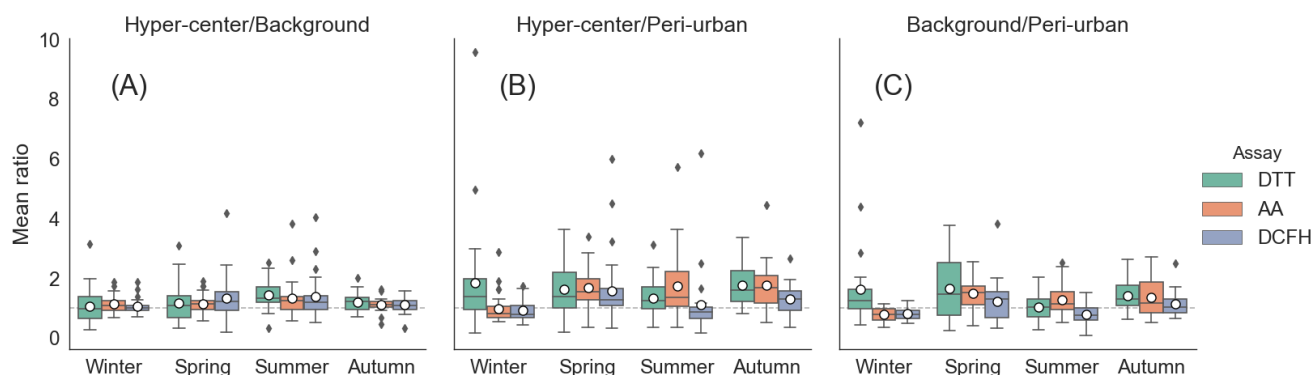
rather than PM_{10} mass concentration. On the other hand, both OP^{AA} ($r=0.76$) and OP^{DCFH} ($r=0.70$) showed good correlations between their measures per volume or per mass pointing out their dependency to PM_{10} concentrations and, indeed, a potential stronger influence by meteorological conditions, a key driver for concentrations in Alpine valleys.

3.2 Spatial variation of OP activity

295 The seasonal mean ratios (MR) of OP activities between sites are presented in Figure 3, calculated by averaging the daily ratios of volume-normalized OP activities (OP_v^{DTT} , OP_v^{AA} , and OP_v^{DCFH}) between the sites (Hyper-center/Background (UH/UB), Hyper-center/Peri-urban (UH/PU), and Background/Peri-urban (UB/PU)) by season, where winter is from December to February, spring is from March to May, summer is June to August, and autumn is September to November.

300 Generally, there is spatial homogeneity (MR closer to 1) in OP between the UB and UH sites in line with the findings from the companion paper (Borlaza et al., 2020). Their similarities in terms of PM_{10} sources has been previously attributed to similarities in source contribution not only from common sources (e.g., biomass burning and nitrate-rich) but also in terms of specific local sources in these sites such as primary traffic, mineral dust, and, to a lower extent, the industrial factor. This could be attributed not only to their proximity in terms of geographical location, but also by their resemblance in typology resulting to similarities of both PM_{10} and OP variabilities.

305

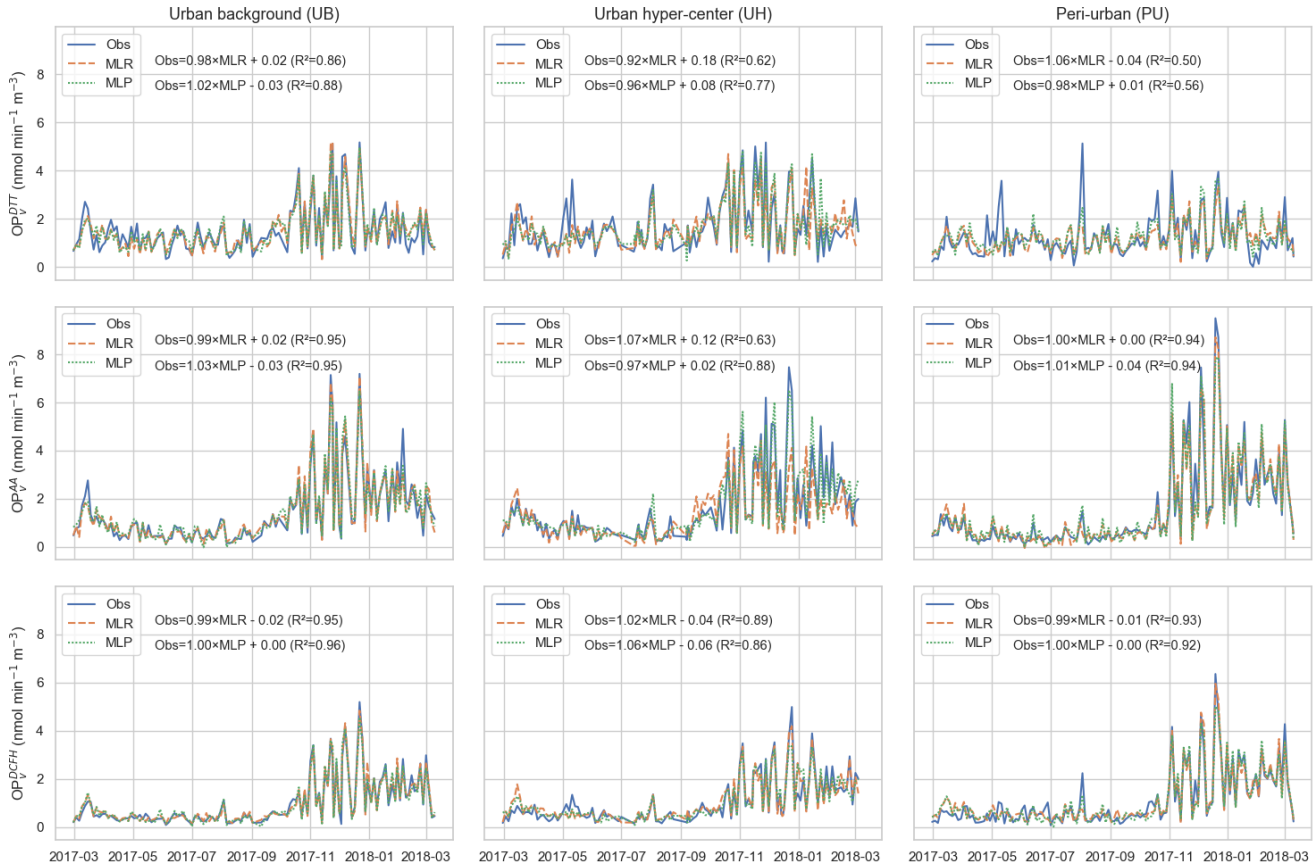


310 **Figure 3: Seasonal mean ratios (MR) between the sites ((A) Hyper-center/Background (UH/UB), (B) Hyper-center/Peri-urban (UH/PU), and (C) Background/Peri-urban (UB/PU)) using volume-normalized OP activities (OP_v^{DTT} , OP_v^{AA} , and OP_v^{DCFH}). Dashed grey line denotes MR equal to 1 suggesting total spatial homogeneity. Boxplot mean marked by white circle and median marked by black line.**

Conversely, there is an observed variability in the MR in UH/PU and UB/PU suggesting weaker homogeneity (MR farther to 1) in the PU site compared to sites closer to the city-center (UH and UB sites). For example, the PU site can be strongly influenced by some event days with extremely low OP_v^{DTT} especially in the winter season ($OP_v^{DTT} < 0.1 \text{ nmol min}^{-1} \text{ m}^{-3}$, $n=3$) resulting to an increase in the MRs against other sites. In fact, the MR for OP_v^{DTT} can be as high as 9.6 and 7.2 during winter for the UH/PU and UB/PU ratio. This can also be seen in the other seasons but more prominent between UH and PU sites. 315 Aside from seasonal influences, there are also some differences between assays as observed in the UH/PU and UB/PU ratio

during winter. For instance, the MRs in OP_v^{DTT} is notably much higher than the in OP_v^{AA} and OP_v^{DCFH} further highlighting assay sensitivity.

320 Although spatial homogeneity was generally observed between the sites, there are local features that must be taken into consideration, as well as seasonal influence and OP assay sensitivity. Overall, there is an observed similarity in the spatiotemporal variabilities of PM_{10} and measured OP activity making it even more interesting to determine which of the PM_{10} sources are driving OP.



325

Figure 4: Comparison of the observed and modelled OP_v (OP_v^{DTT} , OP_v^{AA} , and OP_v^{DCFH}) at different urban sites using MLR and MLP models. The equation of the line and goodness-of-fit (R^2) between observed and modelled OP are included.

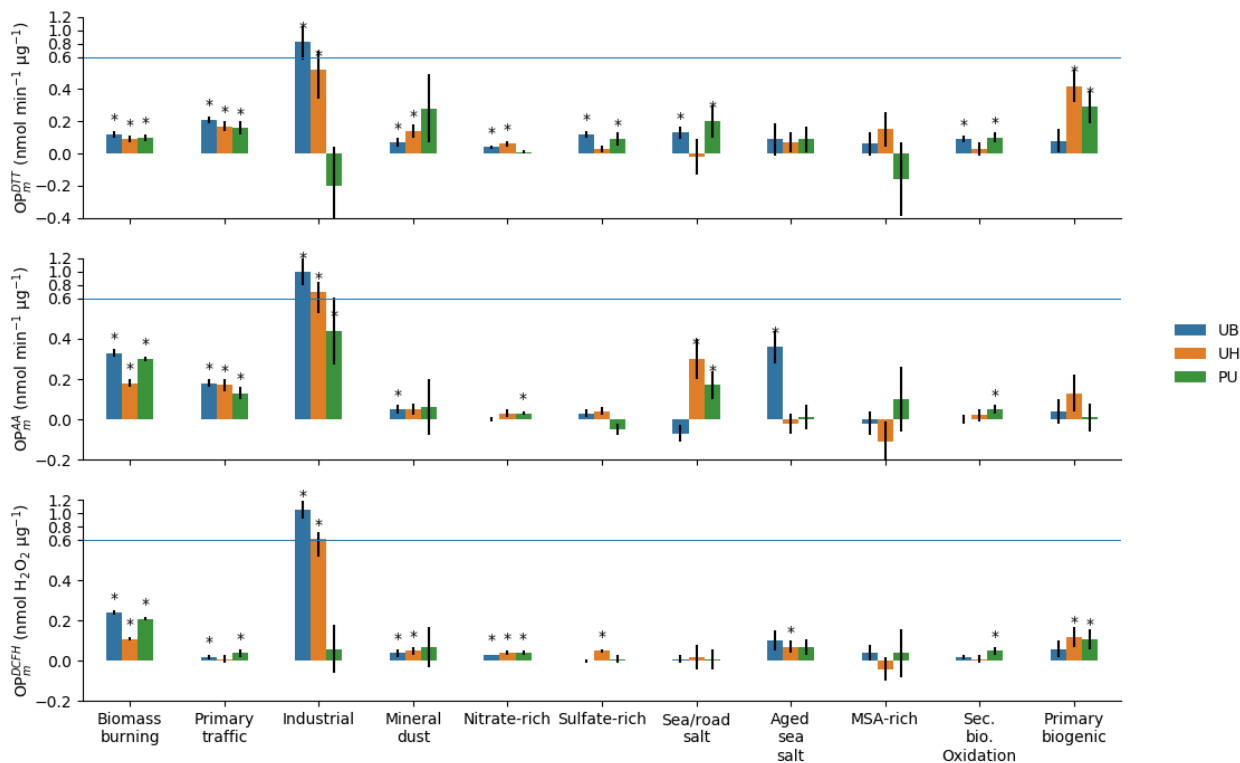
3.3 Determination of the sources driving OP using multiple linear regression (MLR) analysis

To determine the main drivers of the OP of PM₁₀, an OP deconvolution method was performed with a classical MLR analysis following the proposed method by Weber et al. (2018) using the source contributions obtained in the PMF studies presented in the companion paper (Borlaza et al., 2020) and the measured OP at each site.

3.3.1 Performance of the MLR models

Thanks to the OP deconvolution method, the measured OP has been attributed to the PM₁₀ sources allowing the quantification of contribution of each source to OP. Generally, the MLR-modelled OPs are well within range of the observed OP activity, even taking into account the low uncertainties of the measurements as presented in Figure 4. However, there are a few local features (i.e., high OP events) in the observed $OP_v^{D^{TT}}$ during warmer months in the UH and PU sites that were not captured by the MLR models. There are also some over-estimations during the colder months (specifically around January to February 2018) at the same sites. Yet, these lead to an acceptable goodness-of-fit (R^2) for the MLR-modelled $OP_v^{D^{TT}}$ in the UB ($R^2=0.80$), UH ($R^2=0.62$), and PU ($R^2=0.50$) sites, compared to the MLR-modelled OP_v^{AA} (UB: $R^2=0.73$, UH: $R^2=0.63$, and PU: $R^2=0.94$) and OP_v^{DCFH} (UB: $R^2=0.96$, UH: $R^2=0.89$, and PU: $R^2=0.93$). These associations were also confirmed using Pearson correlations (r) as presented in Figure S6 in the supplementary information (S7).

However, there are instances where models, even those with good R^2 -values, could have a considerable bias and should be interpreted with caution. For example, the relationship between the observed and MLR-modelled OP_v^{AA} in the UB site has a slope of 0.9 but an intercept of 0.7, showing significant deviation between model and measured. Additional details on the correlation between the observed and MLR-modelled OP activity are summarized in the supplementary information (S6).



350 **Figure 5: Site-specific intrinsic OP (OP_m) per source analysis from each assay (OP_m^{DTT} , OP_m^{AA} , and OP_m^{DCFH}) represented by mean (bar) and standard deviation (error bar) based on the MLR (Urban background, UB: blue, Urban hyper-center, UH: orange, Peri-urban, PU: green). Note: Asterisks represent statistically significant OP_m within 95% confidence interval ($p\text{-value} \leq 0.05$).**

3.3.2 Intrinsic OP (OP_m) of each PM_{10} source

The ability of each PM source to induce oxidative stress is represented by the intrinsic OP (OP_m) given by the regression coefficient (β) of the MLR model, as shown in Figure 5. With higher OP_m , the source is more redox-active and highly likely to contribute to the overall OP.

355 Generally, the statistically dominant sources (based on the MLR models, $p\text{-value} \leq 0.05$) in every site are the industrial, biomass burning, and primary traffic (except for OP_m^{DCFH} in the UH site) sources, suggesting stronger impact of anthropogenic sources. Both the biomass burning and primary traffic sources have mostly showed significant positive OP_m across all sites. However, amongst the sources with dominant intrinsic OP, it is important to note the variability of the OP_m of the industrial source. This source has been previously identified as a heterogeneous source in the companion paper. It is important to note that the impact of trace metals, used to identify this source (i.e., As, Cd, Cr, Mn, Mo, Ni, Pb, Zn), is inherently variable at this spatial scale.

360 Particularly, the industrial source has the highest OP_m for both UB ($OP_m^{DTT} = 0.82 \pm 0.24$, $p \leq 0.01$; $OP_m^{AA} = 0.99 \pm 0.20$, $p \leq 0.01$; $OP_m^{DCFH} = 1.05 \pm 0.13$, $p \leq 0.01$) and UH ($OP_m^{DTT} = 0.52 \pm 0.18$, $p \leq 0.01$; $OP_m^{AA} = 0.69 \pm 0.16$, $p \leq 0.01$; $OP_m^{DCFH} = 0.62 \pm 0.10$, $p \leq 0.01$) sites. However, for the PU site, the industrial source has a low to negative OP_m for DTT and DCFH assays suggesting that this

source has less impact on this specific urban typology. In fact, in the PU site, the highest OP_m was found in different sources, such as the primary biogenic ($OP_m^{DTT} = 0.29 \pm 0.1$, $p \leq 0.01$), industrial ($= 0.44 \pm 0.17$, $p \leq 0.01$), and biomass burning ($OP_m^{DCFH} = 0.21 \pm 0.01$, $p \leq 0.01$) sources for DTT, AA, and DCFH assays, respectively.

Although it is clear that anthropogenic sources have higher OP_m , there are also impacts from biogenic sources (both primary and secondary biogenic oxidation) that need be considered especially in sites that have an abundance of this type of source. The secondary biogenic oxidation source has only shown statistically significant OP_m in the PU site for all OP assays (also UB site on OP_m^{DTT} only) underlining the influence of site-specific features on OP_m .

Aside from biogenic sources, thanks to the enhanced PMF solution used in this study, we were able to determine the redox characteristics of commonly unresolved sources. The contributions of specific organic tracers (particularly phthalic acid) in some anthropogenic-derived sources, such as sulfate- and nitrate-rich sources, can also point to contributions from anthropogenic secondary organic aerosols (SOA) as discussed in the companion paper (Borlaza et al., 2020). This is particularly important especially that such sources could play a key role in the dynamics of OP of PM_{10} (Daellenbach et al., 2020).

It is also interesting that biomass burning appears to be contributing less to OP_m in the DTT assay compared to both the AA and DCFH assays. We acknowledge the fact that OP from DTT assay has been reported to be responsive/sensitive to organics making this quite intriguing. However, recent studies have reported that OP from DTT assay could be unreactive to some metal species (specifically iron) unlike other assays, namely AA and glutathione (GSH). Hence, OP measured using DTT assay may not completely capture ROS from Fenton chemistry or even the synergistic effects with regards to hydroxyl radical ($\bullet OH$) generation as reported by Xiong et al. (2017). Similarly, Yu et al. (2018) has reported that soluble manganese showed synergistic effects with quinones, while an antagonistic effect between soluble copper and quinones. Generally, there is an undeniable interplay between species that needs to be considered as well as the sensitivity of each assay to species. As much as each analysis attempts to fully characterize the chemistry of PM, there can still be species that are unmeasured but, in fact, play a role in ROS generation. Hence, reported associations could be due to similarity in variations with PM concentration rather than a significant causal relationship between assays and PM components. Nevertheless, the sensitivity of DTT assay to a wider range of compounds that are present in various sources, lead to a more balanced distribution of OP sources (and so weighting the contribution of biomass burning with regards to other sources) than the other OP assays, such as AA and DCFH.

Finally, Weber et al. (2021) discussed the variability of OP at the national scale and the values here are in the ballpark of the national results. A key feature is that the uncertainties of each OP_m can provide information on its statistical significance, therefore offers caution when using these values for modelling purposes.

3.3.3 All-sites average OP contribution (OP_v) by each PM_{10} source

In terms of overall daily mean contribution, as presented in Figure 6 (see supplementary information (S7) for site-specific figures), the main contributors of PM_{10} mass are the biomass burning, and the nitrate- and sulfate-rich sources in the Grenoble basin, when taking into account the results from the 3 sites. However, in terms of OP_v^{DTT} , the primary traffic source showed

the highest contribution ($0.33 \text{ nmol min}^{-1} \text{ m}^{-3}$) closely followed by the biomass burning source ($0.31 \text{ nmol min}^{-1} \text{ m}^{-3}$). For both OP_v^{AA} and OP_v^{DCFH} , the biomass burning source is notably the strongest contributor ($0.72 \text{ nmol min}^{-1} \text{ m}^{-3}$ and $0.56 \text{ nmol min}^{-1} \text{ m}^{-3}$, respectively).

400

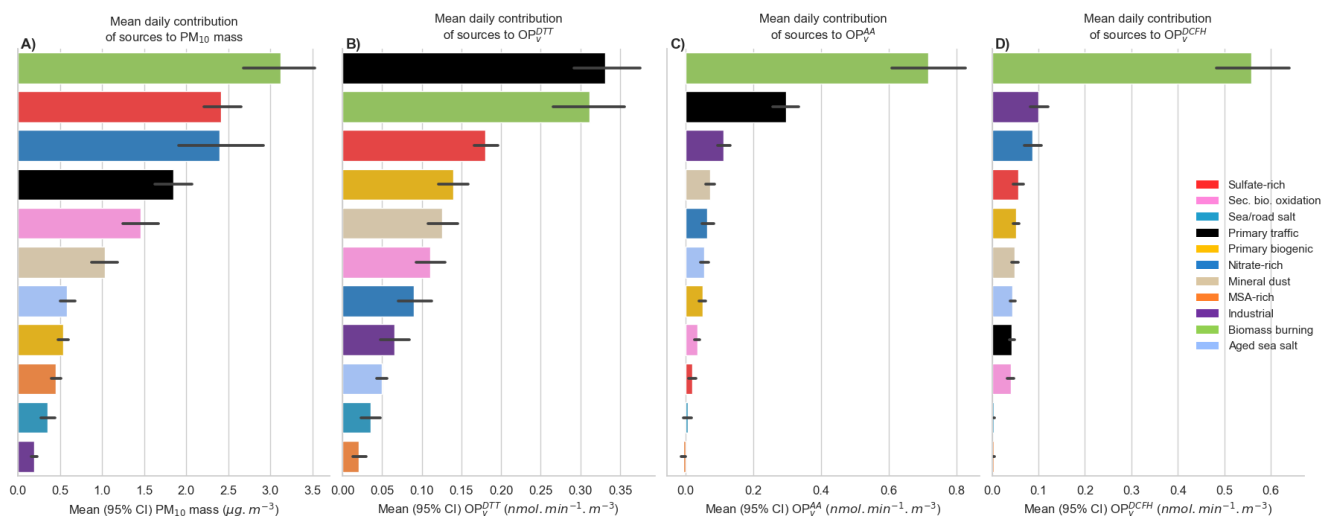


Figure 6: Overall daily mean OP_v contribution of the sources to PM_{10} , OP_v^{DTT} , OP_v^{AA} , and OP_v^{DCFH} using MLR analysis in the form of mean and 95% confident interval of the mean (error bar) (n=378 samples).

The mass contributions of the biomass burning source can be twice as much as that of the primary traffic source, but OP_v contributions in terms of OP_v^{DTT} are almost similar. The industrial source also has very minimal contribution in terms of PM_{10} mass, but has relevant contribution to OP_v . Moreover, there are sources that contribute to a large extent to the total PM_{10} mass but barely contribute to the OP_v , such as the nitrate-rich (all OP_v assays) and sulfate-rich source (only for OP_v^{AA} and OP_v^{DCFH}). This observed redistribution of source impacts based on OP_v highlights the importance of considering PM redox activity instead of solely mass concentration (Daellenbach et al., 2020).

410 Although secondary inorganic sources are commonly associated with low impact on PM toxicity (Cassee et al., 2013; Daellenbach et al., 2020), the sulfate- and nitrate-rich sources showed contributions to OP_v^{DTT} and OP_v^{DCFH} , respectively. Even with minimal OP_m (see Figure 5), the relevant mass contribution of these sources resulted to relevant contribution to OP_v . It should also be considered that both sulfate- and nitrate-rich sources have been previously associated to anthropogenic SOA due to phthalic acid contribution in this factor (Borlaza et al., 2020).

415 Clearly, the OP_v contribution of the biomass burning source is captured by all assays. In fact, in the AA and DCFH assays, the OP_v contributions are both heavily dominated by the biomass burning source, while the DTT assay showed sensitivity to a wider range of sources. However, it is important to take into consideration the mechanism at work behind these assays. Both DTT and AA assays mimic in vivo interactions of redox active components in PM_{10} and biological oxidants representing PM-induced oxidative stress, while DCFH measures generated particle-bound ROS. Although, these source-specific OP_v

420 contributions provide critical knowledge on the main drivers of OP_v , it is difficult to rely on just one measurement (i.e., one type of assay) without testing its relevance to health outcomes.

3.3.4 Seasonal and site-specific differences in OP contribution (OP_v) by each PM_{10} source

Clearly, the previous yearly averages mask strong seasonal variabilities as presented in the monthly OP_v contributions of each source (see Figure 7). During colder months, the OP_v of the biomass burning source is present in all assays and especially prominent in the AA and DCFH assays. During warmer months, the source OP_v contributions varies across different assays. However, the OP_v contributions from the primary traffic source is present throughout the year. Aside from seasonal influences, there are also differences between the sites, that varies according to the assay.

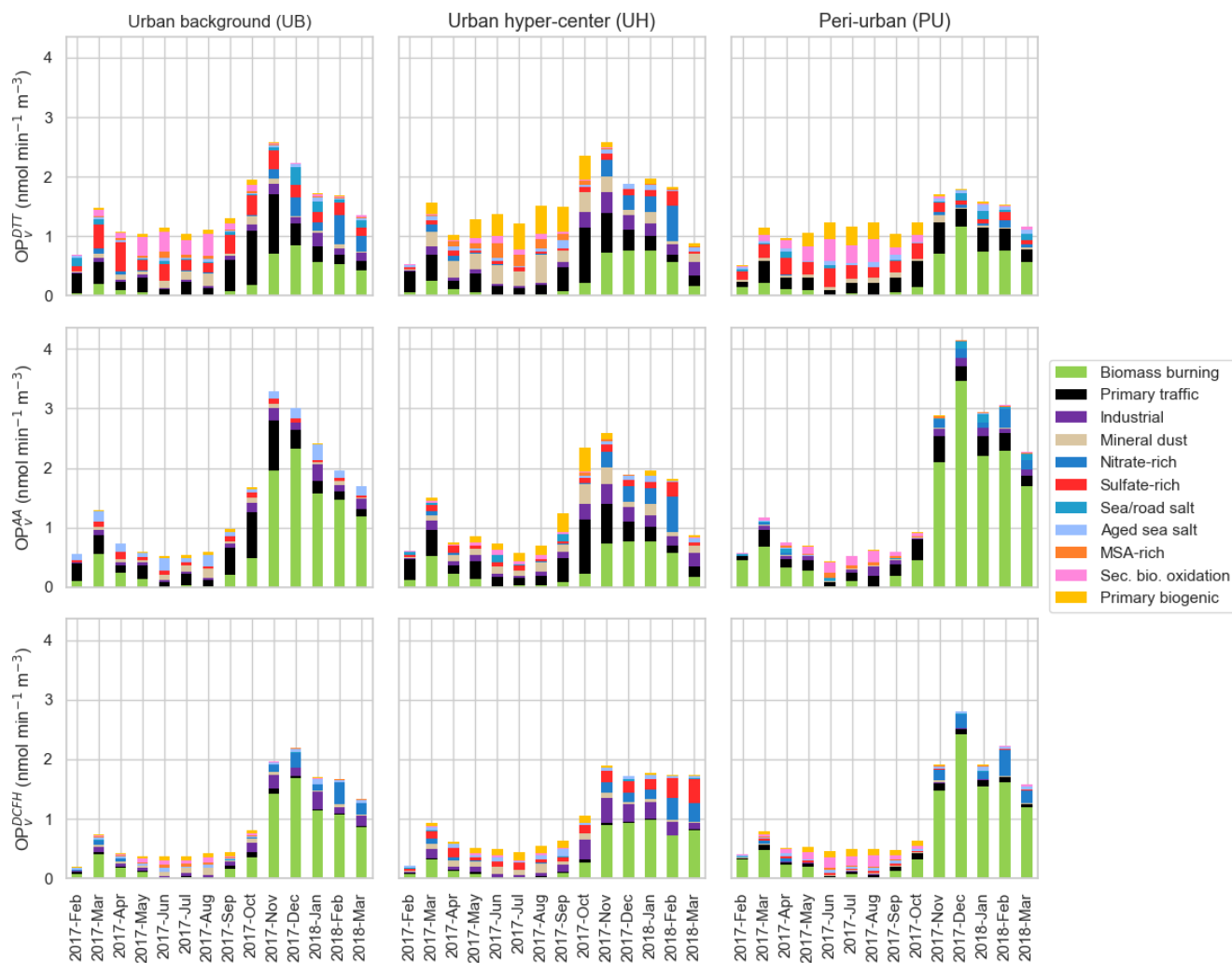
For OP_v^{DTT} , there are similarities in the contributions of some sources in the UB and PU sites such as the consistent monthly contribution from the sulfate-rich source and the contributions from the secondary biogenic source during warmer months highlighting the influence of secondary aerosols in these sites. The UB and UH sites also have similarities in terms of OP_v^{DTT} contributions from the mineral dust source during warmer months and from the nitrate-rich source during the colder months, both of which are sources that can be influenced by road emissions and anthropogenic SOA. This can be explained by the proximity of the UB and UH sites to road ways, where PM_{10} in these sites are more inclined to interact with metals from road dust resuspension and other non-exhaust vehicular emissions than the PU site (discussed in detail in the companion paper (Borlaza et al., 2020)). Surprisingly, there is also a similarity seen in the UH and PU sites in terms of OP_v^{DTT} contributions from the primary biogenic source during warmer months.

For OP_v^{AA} , the contribution from the mineral dust source during warmer months in the UB and UH sites and the contribution from secondary biogenic oxidation source in the PU site were similarly captured. During colder months, biomass burning is dominating in the UB and PU sites, however the UH site exhibited contributions from a variety of sources. There is also a consistent OP_v^{AA} contribution of aged sea salt in the UB site and the contribution of nitrate-rich and sea/road salt during the colder months in the PU site.

For OP_v^{DCFH} , the contributions from the primary traffic source (especially in the UB and PU sites) is much less than the two other assays suggesting weaker sensitivity of DCFH assay to this source. Instead, the contributions from the nitrate-rich source, a source also commonly associated with secondary anthropogenic emissions (Aksoyoglu et al., 2017; Boyd et al., 2017; Faxon et al., 2018; Pennino et al., 2016; Priestley et al., 2018), is more prominent during the colder months in all sites.

These further highlights not only the importance of PM redox activity over mass concentration, but also the importance of considering the seasonal influence to PM sources that drive the OP of PM. These findings are also consistent with current research underlining that the main sources of OP are those including species mainly originating from anthropogenic emissions (Janssen et al., 2014; Shi et al., 2006; Yang et al., 2015) such as road transport and biomass burning (Boogaard et al., 2012; Borlaza et al., 2018; Calas et al., 2019a; Daellenbach et al., 2020; Daher et al., 2014; Pant et al., 2015; Park et al., 2018; Seo

et al., 2020; Simonetti et al., 2018; Weber et al., 2021) and also site typologies that favour the accumulation of pollutants and photo-active aging (Daellenbach et al., 2020; Janssen et al., 2014; Pietrogrande et al., 2019).



455 **Figure 7: The monthly mean OP_v contributions of each PM_{10} source in the three urban sites in Grenoble, France for OP_v^{DTT} , OP_v^{AA} , and OP_v^{CFH} based on MLR analysis.**

3.4 Predicting OP activity from PM_{10} sources using MLP analysis

The residuals between the observed and the MLR-modelled OP could be accounted to atmospheric processes that were not captured as most linear models assume no interaction between independent variables (i.e., multicomponent or multisource interactions). With this in mind, we are inclined to explore another method of predicting OP from PM_{10} sources that hopefully

460

addresses this limitation. The application of ANN techniques using non-linear functions, such as MLP analysis, is an interesting new approach that accounts for correlation and/or non-linear interactions between independent variables.

3.4.1 Optimization of the MLP neural network architecture

A number of MLP architectures (8 architectures in each site (total of 24 MLP models)) were explored to find the optimal neural network in each site by exploring two different activation functions (Hyperbolic tangent (TanH) and Sigmoid), optimization algorithm (Scaled conjugate and Gradient descent), and different learning rates (from 0.2 to 0.6). In the supplementary information (S3), Table S3 shows the performance comparison of all of the MLP models tested. The optimal model was selected based on the lowest RMSE (ideally nearly 0) and highest Pearson correlation coefficient (r) (ideally nearly 1). Other model performance measures such as mean absolute error (MAE), mean absolute percentage error (MAPE), and Spearman rank correlation coefficient (r_s) were also explored and lead to relatively similar results.

It is important to note that, although there are other more complex architectures, we limited our tests to a rudimentary MLP architecture that is deemed sufficient and appropriate based on the type of input and output dataset of this study. Clearly, there is room for further exploration in the direction of using MLP for predicting OP from PM sources. To our knowledge, this is the first attempt to use MLP on apportioning OP from PM sources and may serve as a baseline for future applications of MLP in PM toxicity.

3.4.2 Comparison of predictive accuracy between MLP and MLR models

To conduct insightful evaluation of the predictive accuracy of the MLP and MLR models, the model performance measures were calculated as shown in Table 1. The predicted OP_v^{DTT} by the MLP model generally showed lower prediction error (RMSE) than the MLR model for all the sites. Conversely, the model performance measures in OP_v^{AA} and OP_v^{DCFH} were less straightforward. The predicted OP_v^{AA} showed lower prediction errors for the UB and UH site using MLP models, while lower prediction errors for the PU site using MLR models.

Table 1: The comparison of predictive accuracy of the observed OP activity between the MLR and MLP models based on root mean square error (RMSE) and Pearson correlation (r). Note: RMSE is ideally ~0 (lower RMSE in bold), r is ideally ~1 (higher r in bold).

Site	Model	Root mean square error (RMSE)			Pearson Correlation coefficient (r)		
		OP_v^{DTT}	OP_v^{AA}	OP_v^{DCFH}	OP_v^{DTT}	OP_v^{AA}	OP_v^{DCFH}
Urban background (UB)	MLP	0.35	0.32	0.19	0.94	0.97	0.98
	MLR	0.38	0.32	0.21	0.93	0.97	0.98
Urban hyper-center (UH)	MLP	0.54	0.50	0.30	0.88	0.94	0.95
	MLR	0.69	0.90	0.31	0.79	0.80	0.94
Peri-urban (PU)	MLP	0.58	0.44	0.32	0.75	0.97	0.96
	MLR	0.62	0.42	0.31	0.71	0.97	0.96

485

The temporal distribution of the observed and modelled OP activities for both MLR and MLP models were previously presented in Figure 4. It is interesting to note that even MLP was not able to fully capture some peaks (especially in the warmer months) of the observed OP_v^{DTT} . However, the RMSE values using MLP were much lower than MLR, particularly in the UH site where the RMSE was reduced from 0.69 to 0.54, and in the PU site from 0.62 to 0.58. In the UB site, the MLP did not exceed the performance of MLR by a weighty extent. Nonetheless, the MLP model generally performed better making it a competitive new technique in predicting OP activity even with a rudimentary MLP architecture.

3.4.3 The non-linearity of OP contributions of PM_{10} sources based on MLP analysis

With some interactions between PM_{10} sources resulting to synergistic or antagonistic effects on the OP activity, it is deemed essential to look closer into this potential non-linear aspect to understand better the oxidizing capacity of PM_{10} sources. To demonstrate this non-linearity, the MLP models were applied to dummy datasets leading to source-specific OP_v . The total source-specific OP_v (MLP_{sum} , see section 2.4.3.2) was compared to the original MLP-modelled OP_v as presented in Figure 8 for the OP_v^{DTT} in the UH site (see supplementary information (S7) for similar figures for the UB and PU sites). The data points below the 1:1 line shows an overall synergistic effect between PM_{10} sources on OP_v , while data points above the 1:1 line shows an overall antagonistic effect between PM_{10} sources on OP_v .

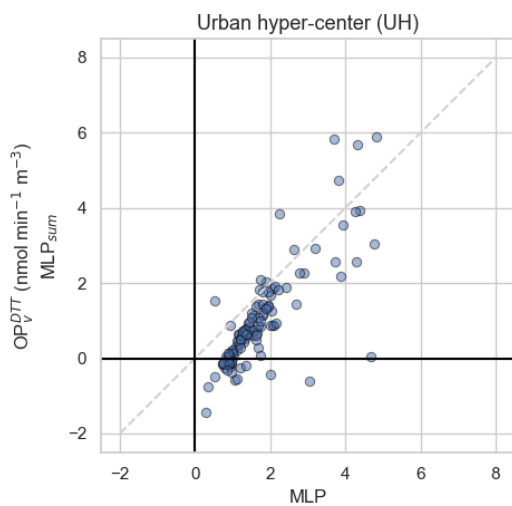


Figure 8: The comparison of the original modelled OP_v^{DTT} (MLP) and the sum of source-specific modelled OP_v^{DTT} activity. Note: Dashed grey line corresponds to the 1:1 line. Data points below the 1:1 line shows an overall synergistic effect between PM_{10} sources on OP activity, above the 1:1 line is otherwise.

Overall, there is a synergistic effect of PM_{10} sources on OP_v^{DTT} in most days in the UH site. This is also seen in the OP_v^{AA} and OP_v^{DCFH} (see Figure S9 in the supplementary information (S8)). Several studies have reported synergistic effects in OP due to the interaction between metal and organic species (Arangio et al., 2016; Charrier and Anastasio, 2015; Dou et al., 2015; Fang

et al., 2017; Li et al., 2012; Lin and Yu, 2020; Xiong et al., 2017; Yu et al., 2018). The UH site has pertinent contributions coming from the mineral dust source (high in metal species, possibly combined with anthropogenic organics, from road dust resuspension) and primary biogenic source (high in organic species) which could be initiating the synergistic effects (see Figure S7 in the supplementary information (S8)). While there are relevant contributions from biogenic sources in the other two sites, their mineral dust source is not as high as in the UH site (or vice versa). These findings further support the importance of accounting the contribution of biogenic sources as previously reported in other similar studies (Samake et al., 2017; Tuet et al., 2017) as well as the importance of source interactions and dynamics as it could have considerable influence on the OP of PM₁₀.

In section 3.4.2, it was presented that MLP offered improvements compared to MLR, based on its much lower prediction errors in the UH site (see Table 1). Indeed, it is possible that MLR had difficulties to generate an accurate OP model for a site that has a highly non-linear behaviour based on the potential synergistic effects between PM₁₀ sources. In fact, the lowest prediction error by MLR (OP_v^{DTT} model in the PU site with RMSE=0.21, see Table 1) also showed data points closer to the 1:1 line between the MLP vs MLP_{sum} (see Figure S9 in the supplementary information (S8)) suggesting weaker influence of the synergistic/antagonistic effects between PM₁₀ sources. However, the MLP still performed better (OP_v^{DTT} model in the PU site with RMSE=0.19, see Table 1) supporting the flexibility of MLP in both linear and non-linear behaviour of PM₁₀ sources compared to MLR.

4 Conclusion

This study, together with the findings of its companion paper (Borlaza et al., 2020), have presented an extensive analysis of a city-scale OP and its association to various sources of PM₁₀ based on a one-year PM₁₀ sampling over different sites in Grenoble (France), with approaches using both linear and non-linear modelling techniques. The main findings of this study are as follows:

- There is a strong seasonality in the observed OP found in all assays used (AA, DTT, and DCFH), with higher OP during colder months and lower OP during warmer months.
- There is a notable spatial difference in OP in a suburban typology against sites closer to the city-center.
- There is an overall agreement (spatiotemporal homogeneity) between the 3 sites in the Grenoble basin, however, there are some influences from local features and site-specific events due to specific sources' contribution.
- The OP of PM₁₀ has been successfully attributed to PMF-resolved sources using Multiple Linear Regression analysis with mostly good model fit.
- The sources of OP with highest redox characteristics (i.e., intrinsic OP or OP_m) are mainly anthropogenic sources such as industrial, primary traffic, and biomass burning sources. The redox characteristics of commonly unresolved sources in the biogenic fraction (MSA-rich, primary biogenic, and secondary biogenic oxidation) were also obtained and such natural sources also contribute to the overall OP during mild seasons.

- 540
- There is a redistribution of the impacts in terms of source OP_v contributions compared to mass contributions, highlighting the importance of considering redox activity over mass concentration in Air Quality policies.
 - There are seasonal influences on sources contributing to OP. During the colder months, the biomass burning source is typically the strongest contributor to all OP. During the warmer months, there are different sources (mineral dust, primary biogenic, secondary biogenic oxidation) contributing to OP in each site. However, there is a consistent
- 545
- contribution from the primary traffic source during the overall year.
 - Even with a rudimentary design, the Multilayer Perceptron approach successfully modelled OP based on PMF-resolved sources, with some improvements on model performance (lower prediction errors, higher association to observed OP) compared to MLR.
 - The MLP also offered improvements especially in sites where there are prominent synergistic and/or antagonistic
- 550
- effects between PM_{10} sources supporting the capabilities of MLP in capturing non-linearities in OP.

Finally, in this paper, we tested for the very first time the use of neural network analysis to apportion OP sources from PM_{10} . We showed that such methodology is at least as robust as the linear classical inversion one and permits an improvement in the OP prediction when local features or non-linear effects occur. This study also demonstrated that enhanced-PMF solution allows to show differences in the spatiotemporal distribution of OP activity, targeting the responsible sources, at a city-scale. These

555 findings pave the way of establishing exposure in homogenous OP areas.

Code availability

The software code is available upon request.

560 Date availability

The chemical, PMF, and OP datasets are available upon request.

Authors contributions

GU, and JLJ designed the atmospheric chemistry part of the MobilAir and QUAMECS program and the whole Get OP stand

565 OP project. SM and CT supervised the sampling at the 3 sites for Atmo AuRA. AA is involved in the CARA program that allows the collection of samples from Les Frênes site. SH is developing OP assays for the group LJSB and SW processed the data. SW developed some of the tools and ideas for in-depth PMF analysis. LJSB, SW, wrote the paper. JLJ and GU revised the original draft. All authors reviewed and edited the manuscript.

570 Competing interests

The authors declare that they have no conflict of interest.

Acknowledgements

The authors would like to kindly thank the dedicated efforts of many people from Atmo-AuRA at the sampling sites, and in the lab at IGE (Anthony Vella, Claire Vérin, Céline Voiron, Rhabira El Azzouzi, and Armelle Crouzet) for collecting and analysing the samples, respectively.

Financial support

This work is supported by the French National Research Agency in the framework of the "Investissements d'avenir" program (ANR-15-IDEX-02), for the MobilAir program and ANR Get OP Stand OP (ANR-19-CE34-0002-01). It also received support from the program QAMECS funded by ADEME (convention 1662C0029), and from LCSQA and French Ministry of Environment for part of the analyses for the Les Frenes site within the CARA program. Chemical analysis on the Air-O-Sol facility at IGE was made possible with the funding of some of the equipment by the Labex OSUG@2020 (ANR10 LABX56). The PhD of SW is funded by ENS Paris. The internship of T Cañete is taking place within the Erasmus exchange program.

References

- Abderrahim, H., Chellali, M. R., and Hamou, A.: Forecasting PM10 in Algiers: efficacy of multilayer perceptron networks, *Environ Sci Pollut Res*, 23, 1634–1641, <https://doi.org/10.1007/s11356-015-5406-6>, 2016.
- Aksoyoglu, S., Ciarelli, G., El-Haddad, I., Baltensperger, U., and Prévôt, A. S. H.: Secondary inorganic aerosols in Europe: sources and the significant influence of biogenic VOC emissions, especially on ammonium nitrate, *Atmos. Chem. Phys.*, 17, 7757–7773, <https://doi.org/10.5194/acp-17-7757-2017>, 2017.
- Arangio, A. M., Tong, H., Socorro, J., Pöschl, U., and Shiraiwa, M.: Quantification of environmentally persistent free radicals and reactive oxygen species in atmospheric aerosol particles, *Atmos. Chem. Phys.*, 16, 13105–13119, <https://doi.org/10.5194/acp-16-13105-2016>, 2016.
- Argyropoulos, G., Basis, A., Voutsas, D., Samara, C., Sowlat, M. H., Hasheminassab, S., and Sioutas, C.: Source apportionment of the redox activity of urban quasi-ultrafine particles (PM_{0.49}) in Thessaloniki following the increased biomass burning due to the economic crisis in Greece, *Science of The Total Environment*, 568, 124–136, <https://doi.org/10.1016/j.scitotenv.2016.05.217>, 2016.
- Ayres, J. G., Borm, P., Cassee, F. R., Castranova, V., Donaldson, K., Ghio, A., Harrison, R. M., Hider, R., Kelly, F., Kooter, I. M., Marano, F., Maynard, R. L., Mudway, I., Nel, A., Sioutas, C., Smith, S., Baeza-Squiban, A., Cho, A., Duggan, S., and Froines, J.: Evaluating the Toxicity of Airborne Particulate Matter and Nanoparticles by Measuring Oxidative Stress Potential—A Workshop Report and Consensus Statement, *Inhalation Toxicology*, 20, 75–99, <https://doi.org/10.1080/08958370701665517>, 2008.
- Bates, J. T., Weber, R. J., Abrams, J., Verma, V., Fang, T., Klein, M., Strickland, M. J., Sarnat, S. E., Chang, H. H., Mulholland, J. A., Tolbert, P. E., and Russell, A. G.: Reactive Oxygen Species Generation Linked to Sources of Atmospheric Particulate Matter and Cardiorespiratory Effects, *Environ. Sci. Technol.*, 49, 13605–13612, <https://doi.org/10.1021/acs.est.5b02967>, 2015.

- 605 Bates, J. T., Fang, T., Verma, V., Zeng, L., Weber, R. J., Tolbert, P. E., Abrams, J. Y., Sarnat, S. E., Klein, M., Mulholland, J. A., and Russell, A. G.: Review of Acellular Assays of Ambient Particulate Matter Oxidative Potential: Methods and Relationships with Composition, Sources, and Health Effects, *Environ. Sci. Technol.*, 53, 4003–4019, <https://doi.org/10.1021/acs.est.8b03430>, 2019.
- 610 Baulig, A., Garlatti, M., Bonvallot, V., Marchand, A., Barouki, R., Marano, F., and Baeza-Squiban, A.: Involvement of reactive oxygen species in the metabolic pathways triggered by diesel exhaust particles in human airway epithelial cells, *American Journal of Physiology-Lung Cellular and Molecular Physiology*, 285, L671–L679, <https://doi.org/10.1152/ajplung.00419.2002>, 2003.
- 615 Belis, C. A., Pikridas, M., Lucarelli, F., Petralia, E., Cavalli, F., Calzolari, G., Berico, M., and Sciare, J.: Source apportionment of fine PM by combining high time resolution organic and inorganic chemical composition datasets, *Atmospheric Environment: X*, 3, 100046, <https://doi.org/10.1016/j.aeaoa.2019.100046>, 2019.
- Bell, M. L. and HEI Health Review Committee: Assessment of the health impacts of particulate matter characteristics, *Res Rep Health Eff Inst*, 5–38, 2012.
- Bengio, Y., Simard, P., and Frasconi, P.: Learning long-term dependencies with gradient descent is difficult, *IEEE Trans. Neural Netw.*, 5, 157–166, <https://doi.org/10.1109/72.279181>, 1994.
- 620 Bessagnet, B., Menut, L., Lapere, R., Couvidat, F., Jaffrezo, J.-L., Mailler, S., Favez, O., Pennel, R., and Siour, G.: High Resolution Chemistry Transport Modeling with the On-Line CHIMERE-WRF Model over the French Alps—Analysis of a Feedback of Surface Particulate Matter Concentrations on Mountain Meteorology, *Atmosphere*, 11, 565, <https://doi.org/10.3390/atmos11060565>, 2020.
- 625 Bishop, C. M.: *Neural networks for pattern recognition*, Clarendon Press ; Oxford University Press, Oxford : New York, 482 pp., 1995.
- Boogaard, H., Janssen, N. A. H., Fischer, P. H., Kos, G. P. A., Weijers, E. P., Cassee, F. R., van der Zee, S. C., de Hartog, J. J., Brunekreef, B., and Hoek, G.: Contrasts in Oxidative Potential and Other Particulate Matter Characteristics Collected Near Major Streets and Background Locations, *Environmental Health Perspectives*, 120, 185–191, <https://doi.org/10.1289/ehp.1103667>, 2012.
- 630 Boppana, V. B. L., Wise, D. J., Ooi, C. C., Zhmayev, E., and Poh, H. J.: CFD assessment on particulate matter filters performance in urban areas, *Sustainable Cities and Society*, 46, 101376, <https://doi.org/10.1016/j.scs.2018.12.004>, 2019.
- Borlaza, L. J. S., Cosep, E. M. R., Kim, S., Lee, K., Joo, H., Park, M., Bate, D., Cayetano, M. G., and Park, K.: Oxidative potential of fine ambient particles in various environments, *Environmental Pollution*, 243, 1679–1688, <https://doi.org/10.1016/j.envpol.2018.09.074>, 2018.
- 635 Borlaza, L. J. S., Weber, S., Uzu, G., Jacob, V., Canete, T., Favez, O., Micallef, S., Trebuchon, C., Slama, R., and Jaffrezo, J.-L.: Disparities in particulate matter (PM10) origins and oxidative potential at a city-scale (Grenoble, France) - Part I: Source apportionment at three neighbouring sites, 2020.
- 640 Boyd, C. M., Nah, T., Xu, L., Berkemeier, T., and Ng, N. L.: Secondary Organic Aerosol (SOA) from Nitrate Radical Oxidation of Monoterpenes: Effects of Temperature, Dilution, and Humidity on Aerosol Formation, Mixing, and Evaporation, *Environ. Sci. Technol.*, 51, 7831–7841, <https://doi.org/10.1021/acs.est.7b01460>, 2017.

- Brown, S. G., Eberly, S., Paatero, P., and Norris, G. A.: Methods for estimating uncertainty in PMF solutions: Examples with ambient air and water quality data and guidance on reporting PMF results, *Science of The Total Environment*, 518–519, 626–635, <https://doi.org/10.1016/j.scitotenv.2015.01.022>, 2015.
- 645 Cabaneros, S. M., Calautit, J. K., and Hughes, B. R.: A review of artificial neural network models for ambient air pollution prediction, *Environmental Modelling & Software*, 119, 285–304, <https://doi.org/10.1016/j.envsoft.2019.06.014>, 2019.
- Cabaneros, S. M., Calautit, J. K., and Hughes, B.: Short- and long-term forecasting of ambient air pollution levels using wavelet-based non-linear autoregressive artificial neural networks with exogenous inputs, *Int. J. EI*, 3, 143–154, <https://doi.org/10.2495/EI-V3-N2-143-154>, 2020.
- 650 Cabaneros, S. M. S., Calautit, J. K. S., and Hughes, B. R.: Hybrid Artificial Neural Network Models for Effective Prediction and Mitigation of Urban Roadside NO₂ Pollution, *Energy Procedia*, 142, 3524–3530, <https://doi.org/10.1016/j.egypro.2017.12.240>, 2017.
- Calas, A., Uzu, G., Martins, J. M. F., Voisin, D., Spadini, L., Lacroix, T., and Jaffrezo, J.-L.: The importance of simulated lung fluid (SLF) extractions for a more relevant evaluation of the oxidative potential of particulate matter, 7, 11617, <https://doi.org/10.1038/s41598-017-11979-3>, 2017.
- 655 Calas, A., Uzu, G., Kelly, F. J., Houdier, S., Martins, J. M. F., Thomas, F., Molton, F., Charron, A., Dunster, C., Oliete, A., Jacob, V., Besombes, J.-L., Chevrier, F., and Jaffrezo, J.-L.: Comparison between five acellular oxidative potential measurement assays performed with detailed chemistry on PM₁₀ samples from the city of Chamonix (France), *Atmos. Chem. Phys.*, 18, 7863–7875, <https://doi.org/10.5194/acp-18-7863-2018>, 2018.
- 660 Calas, A., Uzu, G., Besombes, J.-L., Martins, J. M. F., Redaelli, M., Weber, S., Charron, A., Albinet, A., Chevrier, F., Brulfert, G., Mesbah, B., Favez, O., and Jaffrezo, J.-L.: Seasonal Variations and Chemical Predictors of Oxidative Potential (OP) of Particulate Matter (PM), for Seven Urban French Sites, 20, 2019a.
- Calas, A., Uzu, G., Besombes, J.-L., Martins, J. M. F., Redaelli, M., Weber, S., Charron, A., Albinet, A., Chevrier, F., Brulfert, G., Mesbah, B., Favez, O., and Jaffrezo, J.-L.: Seasonal Variations and Chemical Predictors of Oxidative Potential (OP) of Particulate Matter (PM), for Seven Urban French Sites, *Atmosphere*, 10, 698, <https://doi.org/10.3390/atmos10110698>, 2019b.
- 665 Calcagno, G., Staiano, A., Fortunato, G., Brescia-Morra, V., Salvatore, E., Liguori, R., Capone, S., Filla, A., Longo, G., and Sacchetti, L.: A multilayer perceptron neural network-based approach for the identification of responsiveness to interferon therapy in multiple sclerosis patients, *Information Sciences*, 180, 4153–4163, <https://doi.org/10.1016/j.ins.2010.07.004>, 2010.
- 670 Cassee, F. R., Héroux, M.-E., Gerlofs-Nijland, M. E., and Kelly, F. J.: Particulate matter beyond mass: recent health evidence on the role of fractions, chemical constituents and sources of emission, *Inhalation Toxicology*, 25, 802–812, <https://doi.org/10.3109/08958378.2013.850127>, 2013.
- CEN: Ambient air - Standard gravimetric measurement method for the determination of the PM₁₀ or PM_{2.5} mass concentration of suspended particulate matter, CEN, Brussels, Belgium, 2014.
- CEN: Ambient air - Standard method for measurement of NO₃⁻, SO₄²⁻, Cl⁻, NH₄⁺, Na⁺, K⁺, Mg²⁺, Ca²⁺ in PM_{2.5} as deposited on filters, CEN, Brussels, Belgium, 2017.
- 675 Cesari, D., Merico, E., Grasso, F. M., Decesari, S., Belosi, F., Manarini, F., De Nuntis, P., Rinaldi, M., Volpi, F., Gambaro, A., Morabito, E., and Contini, D.: Source Apportionment of PM_{2.5} and of its Oxidative Potential in an Industrial Suburban Site in South Italy, *Atmosphere*, 10, 758, <https://doi.org/10.3390/atmos10120758>, 2019.

- 680 Chaloulakou, A., Grivas, G., and Spyrellis, N.: Neural Network and Multiple Regression Models for PM₁₀ Prediction in Athens: A Comparative Assessment, *Journal of the Air & Waste Management Association*, 53, 1183–1190, <https://doi.org/10.1080/10473289.2003.10466276>, 2003.
- Charrier, J. G. and Anastasio, C.: Rates of Hydroxyl Radical Production from Transition Metals and Quinones in a Surrogate Lung Fluid, *Environ Sci Technol*, 49, 9317–9325, <https://doi.org/10.1021/acs.est.5b01606>, 2015.
- 685 Charron, A., Polo-Rehn, L., Besombes, J.-L., Golly, B., Buisson, C., Chanut, H., Marchand, N., Guillaud, G., and Jaffrezo, J.-L.: Identification and quantification of particulate tracers of exhaust and non-exhaust vehicle emissions, *Atmos. Chem. Phys.*, 19, 5187–5207, <https://doi.org/10.5194/acp-19-5187-2019>, 2019.
- Chattopadhyay, S. and Bandyopadhyay, G.: Artificial neural network with backpropagation learning to predict mean monthly total ozone in Arosa, Switzerland, *International Journal of Remote Sensing*, 28, 4471–4482, <https://doi.org/10.1080/01431160701250440>, 2007.
- 690 Cho, A. K., Sioutas, C., Miguel, A. H., Kumagai, Y., Schmitz, D. A., Singh, M., Eiguren-Fernandez, A., and Froines, J. R.: Redox activity of airborne particulate matter at different sites in the Los Angeles Basin, *Environmental Research*, 99, 40–47, <https://doi.org/10.1016/j.envres.2005.01.003>, 2005.
- Conte, E., Canepari, S., Frasca, D., and Simonetti, G.: Oxidative Potential of Selected PM Components, *Proceedings*, 1, 108, <https://doi.org/10.3390/ecas2017-04131>, 2017.
- 695 Crobeddu, B., Aragao-Santiago, L., Bui, L.-C., Boland, S., and Baeza Squiban, A.: Oxidative potential of particulate matter 2.5 as predictive indicator of cellular stress, *Environmental Pollution*, 230, 125–133, <https://doi.org/10.1016/j.envpol.2017.06.051>, 2017.
- Dabass, A., Talbott, E. O., Rager, J. R., Marsh, G. M., Venkat, A., Holguin, F., and Sharma, R. K.: Systemic inflammatory markers associated with cardiovascular disease and acute and chronic exposure to fine particulate matter air pollution (PM_{2.5}) among US NHANES adults with metabolic syndrome, *Environmental Research*, 161, 485–491, <https://doi.org/10.1016/j.envres.2017.11.042>, 2018.
- 700 Daellenbach, K. R., Uzu, G., Jiang, J., Cassagnes, L.-E., Leni, Z., Vlachou, A., Stefenelli, G., Canonaco, F., Weber, S., Segers, A., Kuenen, J. J. P., Schaap, M., Favez, O., Albinet, A., Aksoyoglu, S., Dommen, J., Baltensperger, U., Geiser, M., El Haddad, I., Jaffrezo, J.-L., and Prévôt, A. S. H.: Sources of particulate-matter air pollution and its oxidative potential in Europe, *Nature*, 587, 414–419, <https://doi.org/10.1038/s41586-020-2902-8>, 2020.
- 705 Daher, N., Saliba, N. A., Shihadeh, A. L., Jaafar, M., Baalbaki, R., Shafer, M. M., Schauer, J. J., and Sioutas, C.: Oxidative potential and chemical speciation of size-resolved particulate matter (PM) at near-free-way and urban background sites in the greater Beirut area, *Science of The Total Environment*, 470–471, 417–426, <https://doi.org/10.1016/j.scitotenv.2013.09.104>, 2014.
- 710 David, L. M., Ravishankara, A. R., Kodros, J. K., Pierce, J. R., Venkataraman, C., and Sadavarte, P.: Premature Mortality Due to PM_{2.5} Over India: Effect of Atmospheric Transport and Anthropogenic Emissions, *GeoHealth*, 3, 2–10, <https://doi.org/10.1029/2018GH000169>, 2019.
- Delfino, R. J., Sioutas, C., and Malik, S.: Potential Role of Ultrafine Particles in Associations between Airborne Particle Mass and Cardiovascular Health, *Environmental Health Perspectives*, 113, 934–946, <https://doi.org/10.1289/ehp.7938>, 2005.
- 715 Dhalla, N. S., Temsah, R. M., and Netticadan, T.: Role of oxidative stress in cardiovascular diseases:, *Journal of Hypertension*, 18, 655–673, <https://doi.org/10.1097/00004872-200018060-00002>, 2000.

- Díaz-Robles, L. A., Ortega, J. C., Fu, J. S., Reed, G. D., Chow, J. C., Watson, J. G., and Moncada-Herrera, J. A.: A hybrid ARIMA and artificial neural networks model to forecast particulate matter in urban areas: The case of Temuco, Chile, *Atmospheric Environment*, 42, 8331–8340, <https://doi.org/10.1016/j.atmosenv.2008.07.020>, 2008.
- 720 Dionisio, K. L., Arku, R. E., Hughes, A. F., Vallarino, J., Carmichael, H., Spengler, J. D., Agyei-Mensah, S., and Ezzati, M.: Air pollution in Accra neighborhoods: spatial, socioeconomic, and temporal patterns, *Environ. Sci. Technol.*, 44, 2270–2276, <https://doi.org/10.1021/es903276s>, 2010.
- Donaldson, K., Stone, V., Seaton, A., and MacNee, W.: Ambient Particle Inhalation and the Cardiovascular System: Potential Mechanisms, *Environmental Health Perspectives*, 109, 523, <https://doi.org/10.2307/3454663>, 2001.
- 725 Dorling, S. R., Foxall, R. J., Mandic, D. P., and Cawley, G. C.: Maximum likelihood cost functions for neural network models of air quality data, *Atmospheric Environment*, 37, 3435–3443, [https://doi.org/10.1016/S1352-2310\(03\)00323-6](https://doi.org/10.1016/S1352-2310(03)00323-6), 2003.
- Dou, J., Lin, P., Kuang, B.-Y., and Yu, J. Z.: Reactive Oxygen Species Production Mediated by Humic-like Substances in Atmospheric Aerosols: Enhancement Effects by Pyridine, Imidazole, and Their Derivatives, *Environ. Sci. Technol.*, 49, 6457–6465, <https://doi.org/10.1021/es5059378>, 2015.
- 730 Du, Y., Xu, X., Chu, M., Guo, Y., and Wang, J.: Air particulate matter and cardiovascular disease: the epidemiological, biomedical and clinical evidence, *J Thorac Dis*, 8, E8–E19, <https://doi.org/10.3978/j.issn.2072-1439.2015.11.37>, 2016.
- Elangasinghe, M. A., Singhal, N., Dirks, K. N., and Salmond, J. A.: Development of an ANN-based air pollution forecasting system with explicit knowledge through sensitivity analysis, *Atmospheric Pollution Research*, 5, 696–708, <https://doi.org/10.5094/APR.2014.079>, 2014.
- 735 Eldakhly, N. M., Aboul-Ela, M., and Abdalla, A.: Air Pollution Forecasting Model Based on Chance Theory and Intelligent Techniques, *Int. J. Artif. Intell. Tools*, 26, 1750024, <https://doi.org/10.1142/S0218213017500245>, 2017.
- Etyemezian, V., Tesfaye, M., Yimer, A., Chow, J., Mesfin, D., Nega, T., Nikolich, G., Watson, J., and Wondmagegn, M.: Results from a pilot-scale air quality study in Addis Ababa, Ethiopia, *Atmospheric Environment*, 39, 7849–7860, <https://doi.org/10.1016/j.atmosenv.2005.08.033>, 2005.
- 740 Fang, T., Verma, V., Bates, J. T., Abrams, J., Klein, M., Strickland, M. J., Sarnat, S. E., Chang, H. H., Mulholland, J. A., Tolbert, P. E., Russell, A. G., and Weber, R. J.: Oxidative potential of ambient water-soluble PM_{2.5} in the southeastern United States: contrasts in sources and health associations between ascorbic acid (AA) and dithiothreitol (DTT) assays, *Atmos. Chem. Phys.*, 16, 3865–3879, <https://doi.org/10.5194/acp-16-3865-2016>, 2016.
- 745 Fang, T., Guo, H., Zeng, L., Verma, V., Nenes, A., and Weber, R. J.: Highly Acidic Ambient Particles, Soluble Metals, and Oxidative Potential: A Link between Sulfate and Aerosol Toxicity, *Environ. Sci. Technol.*, 51, 2611–2620, <https://doi.org/10.1021/acs.est.6b06151>, 2017.
- Favez, O., El Haddad, I., Piot, C., Boréave, A., Abidi, E., Marchand, N., Jaffrezo, J.-L., Besombes, J.-L., Personnaz, M.-B., Sciare, J., Wortham, H., George, C., and D’Anna, B.: Inter-comparison of source apportionment models for the estimation of wood burning aerosols during wintertime in an Alpine city (Grenoble, France), *Atmos. Chem. Phys.*, 10, 5295–5314, <https://doi.org/10.5194/acp-10-5295-2010>, 2010.
- 750 Favez, O., Salameh, D., and Jaffrezo, J.-L.: Traitement harmonisé de jeux de données multi-sites pour l’étude de sources de PM par Positive Matrix Factorization (PMF), LCSQA, 2017.

- Faxon, C., Hammes, J., Le Breton, M., Pathak, R. K., and Hallquist, M.: Characterization of organic nitrate constituents of secondary organic aerosol (SOA) from nitrate-radical-initiated oxidation of limonene using high-resolution chemical ionization mass spectrometry, *Atmos. Chem. Phys.*, 18, 5467–5481, <https://doi.org/10.5194/acp-18-5467-2018>, 2018.
- 755 Fontes, T., Silva, L. M., Silva, M. P., Barros, N., and Carvalho, A. C.: Can artificial neural networks be used to predict the origin of ozone episodes?, *Science of The Total Environment*, 488–489, 197–207, <https://doi.org/10.1016/j.scitotenv.2014.04.077>, 2014.
- Gao, D., Ripley, S., Weichenthal, S., and Godri Pollitt, K. J.: Ambient particulate matter oxidative potential: Chemical determinants, associated health effects, and strategies for risk management, *Free Radical Biology and Medicine*, 151, 7–25, 760 <https://doi.org/10.1016/j.freeradbiomed.2020.04.028>, 2020a.
- Gao, D., Mulholland, J. A., Russell, A. G., and Weber, R. J.: Characterization of water-insoluble oxidative potential of PM_{2.5} using the dithiothreitol assay, *Atmospheric Environment*, 224, 117327, <https://doi.org/10.1016/j.atmosenv.2020.117327>, 2020b.
- 765 García Nieto, P. J., Sánchez Lasheras, F., García-Gonzalo, E., and de Cos Juez, F. J.: PM₁₀ concentration forecasting in the metropolitan area of Oviedo (Northern Spain) using models based on SVM, MLP, VARMA and ARIMA: A case study, *Science of The Total Environment*, 621, 753–761, <https://doi.org/10.1016/j.scitotenv.2017.11.291>, 2018.
- Gardner, M. W. and Dorling, S. R.: Artificial neural networks (the multilayer perceptron)—a review of applications in the atmospheric sciences, *Atmospheric Environment*, 32, 2627–2636, [https://doi.org/10.1016/S1352-2310\(97\)00447-0](https://doi.org/10.1016/S1352-2310(97)00447-0), 1998.
- 770 Gerken, W. C., Purvis, L. K., and Butera, R. J.: Genetic algorithm for optimization and specification of a neuron model, *Neurocomputing*, 69, 1039–1042, <https://doi.org/10.1016/j.neucom.2005.12.041>, 2006.
- Gianini, M. F. D., Fischer, A., Gehrig, R., Ulrich, A., Wichser, A., Piot, C., Besombes, J.-L., and Hueglin, C.: Comparative source apportionment of PM₁₀ in Switzerland for 2008/2009 and 1998/1999 by Positive Matrix Factorisation, *Atmospheric Environment*, 54, 149–158, <https://doi.org/10.1016/j.atmosenv.2012.02.036>, 2012.
- 775 Gietl, J. K. and Klemm, O.: Analysis of Traffic and Meteorology on Airborne Particulate Matter in Münster, Northwest Germany, *Journal of the Air & Waste Management Association*, 59, 809–818, <https://doi.org/10.3155/1047-3289.59.7.809>, 2009.
- Grover, B. D.: Measurement of total PM_{2.5} mass (nonvolatile plus semivolatile) with the Filter Dynamic Measurement System tapered element oscillating microbalance monitor, *J. Geophys. Res.*, 110, D07S03, <https://doi.org/10.1029/2004JD004995>, 2005.
- 780 Guo, H., Jin, L., and Huang, S.: Effect of PM characterization on PM oxidative potential by acellular assays: a review, 0, <https://doi.org/10.1515/reveh-2020-0003>, 2020.
- Gupta, P. and Christopher, S. A.: Particulate matter air quality assessment using integrated surface, satellite, and meteorological products: 2. A neural network approach, *J. Geophys. Res.*, 114, D20205, <https://doi.org/10.1029/2008JD011497>, 2009.
- 785 Gurgueira, S. A., Lawrence, J., Coull, B., Murthy, G. G. K., and González-Flecha, B.: Rapid increases in the steady-state concentration of reactive oxygen species in the lungs and heart after particulate air pollution inhalation., *Environmental Health Perspectives*, 110, 749–755, <https://doi.org/10.1289/ehp.02110749>, 2002.

- 790 He, H.-D., Lu, W.-Z., and Xue, Y.: Prediction of particulate matters at urban intersection by using multilayer perceptron model based on principal components, *Stoch Environ Res Risk Assess*, 29, 2107–2114, <https://doi.org/10.1007/s00477-014-0989-x>, 2015.
- Herich, H., Gianini, M. F. D., Piot, C., Močnik, G., Jaffrezo, J.-L., Besombes, J.-L., Prévôt, A. S. H., and Hueglin, C.: Overview of the impact of wood burning emissions on carbonaceous aerosols and PM in large parts of the Alpine region, *Atmospheric Environment*, 89, 64–75, <https://doi.org/10.1016/j.atmosenv.2014.02.008>, 2014.
- 795 Hime, N., Marks, G., and Cowie, C.: A Comparison of the Health Effects of Ambient Particulate Matter Air Pollution from Five Emission Sources, *IJERPH*, 15, 1206, <https://doi.org/10.3390/ijerph15061206>, 2018.
- Hochreiter, S.: The Vanishing Gradient Problem During Learning Recurrent Neural Nets and Problem Solutions, *Int. J. Unc. Fuzz. Knowl. Based Syst.*, 06, 107–116, <https://doi.org/10.1142/S0218488598000094>, 1998.
- Hochreiter, S. and Schmidhuber, J.: Long Short-Term Memory, *Neural Computation*, 9, 1735–1780, <https://doi.org/10.1162/neco.1997.9.8.1735>, 1997.
- 800 Hooyberghs, J., Mensink, C., Dumont, G., Fierens, F., and Brasseur, O.: A neural network forecast for daily average PM concentrations in Belgium, *Atmospheric Environment*, 39, 3279–3289, <https://doi.org/10.1016/j.atmosenv.2005.01.050>, 2005.
- Huang, C.-J. and Kuo, P.-H.: A Deep CNN-LSTM Model for Particulate Matter (PM_{2.5}) Forecasting in Smart Cities, *Sensors*, 18, 2220, <https://doi.org/10.3390/s18072220>, 2018.
- 805 IBM: IBM SPSS Neural Networks 24, https://www.ibm.com/support/knowledgecenter/de/SSLVMB_23.0.0/spss/neural_network/idh_idd_mlp_variables.html, 2016.
- Janssen, N. A. H., Yang, A., Strak, M., Steenhof, M., Hellack, B., Gerlofs-Nijland, M. E., Kuhlbusch, T., Kelly, F., Harrison, R., Brunekreef, B., Hoek, G., and Cassee, F.: Oxidative potential of particulate matter collected at sites with different source characteristics, *Science of The Total Environment*, 472, 572–581, <https://doi.org/10.1016/j.scitotenv.2013.11.099>, 2014.
- 810 Jiang, Ahmed, Canchola, Chen, and Lin: Use of Dithiothreitol Assay to Evaluate the Oxidative Potential of Atmospheric Aerosols, *Atmosphere*, 10, 571, <https://doi.org/10.3390/atmos10100571>, 2019.
- Jiang, D., Zhang, Y., Hu, X., Zeng, Y., Tan, J., and Shao, D.: Progress in developing an ANN model for air pollution index forecast, *Atmospheric Environment*, 38, 7055–7064, <https://doi.org/10.1016/j.atmosenv.2003.10.066>, 2004.
- 815 Jin, X., Xue, B., Zhou, Q., Su, R., and Li, Z.: Mitochondrial damage mediated by ROS incurs bronchial epithelial cell apoptosis upon ambient PM_{2.5} exposure, *J. Toxicol. Sci.*, 43, 101–111, <https://doi.org/10.2131/jts.43.101>, 2018.
- Jovanovic, M. V., Savic, J. Z., Salimi, F., Stevanovic, S., Brown, R. A., Jovasevic-Stojanovic, M., Manojlovic, D., Bartonova, A., Bottle, S., and Ristovski, Z. D.: Measurements of Oxidative Potential of Particulate Matter at Belgrade Tunnel; Comparison of BPEAnit, DTT and DCFH Assays, *IJERPH*, 16, 4906, <https://doi.org/10.3390/ijerph16244906>, 2019.
- 820 Kelly, F. J.: Oxidative stress: its role in air pollution and adverse health effects, *Occupational and Environmental Medicine*, 60, 612–616, <https://doi.org/10.1136/oem.60.8.612>, 2003.
- Kelly, F. J. and Mudway, I. S.: Protein oxidation at the air-lung interface, *Amino Acids*, 25, 375–396, <https://doi.org/10.1007/s00726-003-0024-x>, 2003.

- Kim, M. and Gilley, J. E.: Artificial Neural Network estimation of soil erosion and nutrient concentrations in runoff from land application areas, *Computers and Electronics in Agriculture*, 64, 268–275, <https://doi.org/10.1016/j.compag.2008.05.021>, 2008.
- 825
- Krasnov, H., Kloog, I., Friger, M., and Katra, I.: The Spatio-Temporal Distribution of Particulate Matter during Natural Dust Episodes at an Urban Scale, *PLoS ONE*, 11, e0160800, <https://doi.org/10.1371/journal.pone.0160800>, 2016.
- Kukkonen, J.: Extensive evaluation of neural network models for the prediction of NO₂ and PM₁₀ concentrations, compared with a deterministic modelling system and measurements in central Helsinki, *Atmospheric Environment*, 37, 4539–4550, 830 [https://doi.org/10.1016/S1352-2310\(03\)00583-1](https://doi.org/10.1016/S1352-2310(03)00583-1), 2003.
- Lao, X. Q., Guo, C., Chang, L., Bo, Y., Zhang, Z., Chuang, Y. C., Jiang, W. K., Lin, C., Tam, T., Lau, A. K. H., Lin, C.-Y., and Chan, T.-C.: Long-term exposure to ambient fine particulate matter (PM_{2.5}) and incident type 2 diabetes: a longitudinal cohort study, *Diabetologia*, 62, 759–769, <https://doi.org/10.1007/s00125-019-4825-1>, 2019.
- Leni, Z., Cassagnes, L. E., Daellenbach, K. R., El Haddad, I., Vlachou, A., Uzu, G., Prévôt, A. S. H., Jaffrezo, J.-L., Baumlin, N., Salathe, M., Baltensperger, U., Dommen, J., and Geiser, M.: Oxidative stress-induced inflammation in susceptible airways by anthropogenic aerosol, *PLoS ONE*, 15, e0233425, <https://doi.org/10.1371/journal.pone.0233425>, 2020.
- 835
- Li, Y., Zhu, T., Zhao, J., and Xu, B.: Interactive Enhancements of Ascorbic Acid and Iron in Hydroxyl Radical Generation in Quinone Redox Cycling, *Environ. Sci. Technol.*, 46, 10302–10309, <https://doi.org/10.1021/es301834r>, 2012.
- Lin, M. and Yu, J. Z.: Assessment of Interactions between Transition Metals and Atmospheric Organics: Ascorbic Acid Depletion and Hydroxyl Radical Formation in Organic-Metal Mixtures, *Environ. Sci. Technol.*, 54, 1431–1442, 840 <https://doi.org/10.1021/acs.est.9b07478>, 2020.
- Matus C., P. and Oyarzún G., M.: Impacto del Material Particulado aéreo (MP_{2,5}) sobre las hospitalizaciones por enfermedades respiratorias en niños: estudio caso-control alterno, *Rev Chil Pediatr*, 90, 166, <https://doi.org/10.32641/rchped.v90i2.750>, 2019.
- 845
- McKendry, I. G.: Evaluation of Artificial Neural Networks for Fine Particulate Pollution (PM₁₀ and PM_{2.5}) Forecasting, *Journal of the Air & Waste Management Association*, 52, 1096–1101, <https://doi.org/10.1080/10473289.2002.10470836>, 2002.
- Mudway, I. S., Kelly, F. J., and Holgate, S. T.: Oxidative stress in air pollution research, *Free Radical Biology and Medicine*, 151, 2–6, <https://doi.org/10.1016/j.freeradbiomed.2020.04.031>, 2020.
- 850
- Nathan, N. S., Saravanane, R., and Sundararajan, T.: Application of ANN and MLR Models on Groundwater Quality Using CWQI at Lawspet, Puducherry in India, *GEP*, 05, 99–124, <https://doi.org/10.4236/gep.2017.53008>, 2017.
- Nel, A.: ATMOSPHERE: Enhanced: Air Pollution-Related Illness: Effects of Particles, *Science*, 308, 804–806, <https://doi.org/10.1126/science.1108752>, 2005.
- Norris, G., Duvall, R., Brown, S., and Bai, S.: Positive Matrix Factorization (PMF) 5.0 Fundamentals and User Guide, 136, 855 2014.
- Ordieres, J. B., Vergara, E. P., Capuz, R. S., and Salazar, R. E.: Neural network prediction model for fine particulate matter (PM_{2.5}) on the US–Mexico border in El Paso (Texas) and Ciudad Juárez (Chihuahua), *Environmental Modelling & Software*, 20, 547–559, <https://doi.org/10.1016/j.envsoft.2004.03.010>, 2005.

- 860 Paatero, P.: The Multilinear Engine—A Table-Driven, Least Squares Program for Solving Multilinear Problems, Including the n -Way Parallel Factor Analysis Model, *Journal of Computational and Graphical Statistics*, 8, 854–888, <https://doi.org/10.1080/10618600.1999.10474853>, 1999.
- Padhi, B. K. and Padhy, P. K.: Assessment of intra-urban variability in outdoor air quality and its health risks, *Inhal Toxicol*, 20, 973–979, <https://doi.org/10.1080/08958370701866420>, 2008.
- 865 Pant, P., Baker, S. J., Shukla, A., Maikawa, C., Godri Pollitt, K. J., and Harrison, R. M.: The PM 10 fraction of road dust in the UK and India: Characterization, source profiles and oxidative potential, *Science of The Total Environment*, 530–531, 445–452, <https://doi.org/10.1016/j.scitotenv.2015.05.084>, 2015.
- Papanastasiou, D. K., Melas, D., and Kioutsioukis, I.: Development and Assessment of Neural Network and Multiple Regression Models in Order to Predict PM10 Levels in a Medium-sized Mediterranean City, *Water Air Soil Pollut*, 182, 325–334, <https://doi.org/10.1007/s11270-007-9341-0>, 2007.
- 870 Paraskevopoulou, D., Bougiatioti, A., Stavroulas, I., Fang, T., Lianou, M., Liakakou, E., Gerasopoulos, E., Weber, R., Nenes, A., and Mihalopoulos, N.: Yearlong variability of oxidative potential of particulate matter in an urban Mediterranean environment, *Atmospheric Environment*, 206, 183–196, <https://doi.org/10.1016/j.atmosenv.2019.02.027>, 2019.
- 875 Park, M., Joo, H. S., Lee, K., Jang, M., Kim, S. D., Kim, I., Borlaza, L. J. S., Lim, H., Shin, H., Chung, K. H., Choi, Y.-H., Park, S. G., Bae, M.-S., Lee, J., Song, H., and Park, K.: Differential toxicities of fine particulate matters from various sources, *Sci Rep*, 8, 17007, <https://doi.org/10.1038/s41598-018-35398-0>, 2018.
- Pennino, M. J., Kaushal, S. S., Murthy, S. N., Blomquist, J. D., Cornwell, J. C., and Harris, L. A.: Sources and transformations of anthropogenic nitrogen along an urban river–estuarine continuum, *Biogeosciences*, 13, 6211–6228, <https://doi.org/10.5194/bg-13-6211-2016>, 2016.
- 880 Perez, P. and Reyes, J.: An integrated neural network model for PM10 forecasting, *Atmospheric Environment*, 40, 2845–2851, <https://doi.org/10.1016/j.atmosenv.2006.01.010>, 2006.
- Perrone, M. G., Zhou, J., Malandrino, M., Sangiorgi, G., Rizzi, C., Ferrero, L., Dommen, J., and Bolzacchini, E.: PM chemical composition and oxidative potential of the soluble fraction of particles at two sites in the urban area of Milan, Northern Italy, *Atmospheric Environment*, 128, 104–113, <https://doi.org/10.1016/j.atmosenv.2015.12.040>, 2016.
- 885 Piao, M. J., Ahn, M. J., Kang, K. A., Ryu, Y. S., Hyun, Y. J., Shilnikova, K., Zhen, A. X., Jeong, J. W., Choi, Y. H., Kang, H. K., Koh, Y. S., and Hyun, J. W.: Particulate matter 2.5 damages skin cells by inducing oxidative stress, subcellular organelle dysfunction, and apoptosis, *Arch Toxicol*, 92, 2077–2091, <https://doi.org/10.1007/s00204-018-2197-9>, 2018.
- Pietrogrande, Russo, and Zagatti: Review of PM Oxidative Potential Measured with Acellular Assays in Urban and Rural Sites across Italy, *Atmosphere*, 10, 626, <https://doi.org/10.3390/atmos10100626>, 2019.
- 890 Pietrogrande, M. C., Perrone, M. R., Manarini, F., Romano, S., Udisti, R., and Becagli, S.: PM10 oxidative potential at a Central Mediterranean Site: Association with chemical composition and meteorological parameters, *Atmospheric Environment*, 188, 97–111, <https://doi.org/10.1016/j.atmosenv.2018.06.013>, 2018.
- Pope, C. A., Ezzati, M., and Dockery, D. W.: Fine-Particulate Air Pollution and Life Expectancy in the United States, *N Engl J Med*, 360, 376–386, <https://doi.org/10.1056/NEJMsa0805646>, 2009.
- 895 Pope III, C. A.: Lung Cancer, Cardiopulmonary Mortality, and Long-term Exposure to Fine Particulate Air Pollution, *JAMA*, 287, 1132, <https://doi.org/10.1001/jama.287.9.1132>, 2002.

- Priestley, M., Le Breton, M., Bannan, T. J., Leather, K. E., Bacak, A., Reyes-Villegas, E., De Vocht, F., Shallcross, B. M. A., Brazier, T., Anwar Khan, M., Allan, J., Shallcross, D. E., Coe, H., and Percival, C. J.: Observations of Isocyanate, Amide, Nitrate, and Nitro Compounds From an Anthropogenic Biomass Burning Event Using a ToF-CIMS, *J. Geophys. Res. Atmos.*, <https://doi.org/10.1002/2017JD027316>, 2018.
- 900 Qiao, F., Li, Q., and Lei, Y.: Particulate Matter Caused Health Risk in an Urban Area of the Middle East and the Challenges in Reducing its Anthropogenic Emissions, *Environ Pollut Climate Change*, 02, <https://doi.org/10.4172/2573-458X.1000145>, 2018.
- Rahimi, A.: Short-term prediction of NO₂ and NO_x concentrations using multilayer perceptron neural network: a case study of Tabriz, Iran, *Ecol Process*, 6, 4, <https://doi.org/10.1186/s13717-016-0069-x>, 2017.
- 905 Rohr, A. C. and Wyzga, R. E.: Attributing health effects to individual particulate matter constituents, *Atmospheric Environment*, 62, 130–152, <https://doi.org/10.1016/j.atmosenv.2012.07.036>, 2012.
- Salazar-Ruiz, E., Ordieres, J. B., Vergara, E. P., and Capuz-Rizo, S. F.: Development and comparative analysis of tropospheric ozone prediction models using linear and artificial intelligence-based models in Mexicali, Baja California (Mexico) and Calexico, California (US), *Environmental Modelling & Software*, 23, 1056–1069, <https://doi.org/10.1016/j.envsoft.2007.11.009>, 2008.
- 910 Samake, A., Uzu, G., Martins, J. M. F., Calas, A., Vince, E., Parat, S., and Jaffrezo, J. L.: The unexpected role of bioaerosols in the Oxidative Potential of PM, 7, 10978, <https://doi.org/10.1038/s41598-017-11178-0>, 2017.
- Schwela, D.: Air Pollution and Health in Urban Areas, 15, <https://doi.org/10.1515/REVEH.2000.15.1-2.13>, 2000.
- Seo, I., Lee, K., Bae, M.-S., Park, M., Maskey, S., Seo, A., Borlaza, L. J. S., Cosep, E. M. R., and Park, K.: Comparison of physical and chemical characteristics and oxidative potential of fine particles emitted from rice straw and pine stem burning, *Environmental Pollution*, 267, 115599, <https://doi.org/10.1016/j.envpol.2020.115599>, 2020.
- 915 Shi, T., Duffin, R., Borm, P. J. A., Li, H., Weishaupt, C., and Schins, R. P. F.: Hydroxyl-radical-dependent DNA damage by ambient particulate matter from contrasting sampling locations, *Environmental Research*, 101, 18–24, <https://doi.org/10.1016/j.envres.2005.09.005>, 2006.
- 920 Shiraiwa, M., Ueda, K., Pozzer, A., Lammel, G., Kampf, C. J., Fushimi, A., Enami, S., Arangio, A. M., Fröhlich-Nowoisky, J., Fujitani, Y., Furuyama, A., Lakey, P. S. J., Lelieveld, J., Lucas, K., Morino, Y., Pöschl, U., Takahama, S., Takami, A., Tong, H., Weber, B., Yoshino, A., and Sato, K.: Aerosol Health Effects from Molecular to Global Scales, *Environ. Sci. Technol.*, 51, 13545–13567, <https://doi.org/10.1021/acs.est.7b04417>, 2017.
- Simonetti, G., Conte, E., Perrino, C., and Canepari, S.: Oxidative potential of size-segregated PM in an urban and an industrial area of Italy, *Atmospheric Environment*, 187, 292–300, <https://doi.org/10.1016/j.atmosenv.2018.05.051>, 2018.
- 925 Srivastava, D., Tomaz, S., Favez, O., Lanzafame, G. M., Golly, B., Besombes, J.-L., Alleman, L. Y., Jaffrezo, J.-L., Jacob, V., Perraudin, E., Villenave, E., and Albinet, A.: Speciation of organic fraction does matter for source apportionment. Part 1: A one-year campaign in Grenoble (France), *Science of The Total Environment*, 624, 1598–1611, <https://doi.org/10.1016/j.scitotenv.2017.12.135>, 2018.
- 930 Tomaz, S., Shahpoury, P., Jaffrezo, J.-L., Lammel, G., Perraudin, E., Villenave, E., and Albinet, A.: One-year study of polycyclic aromatic compounds at an urban site in Grenoble (France): Seasonal variations, gas/particle partitioning and cancer risk estimation, *Science of The Total Environment*, 565, 1071–1083, <https://doi.org/10.1016/j.scitotenv.2016.05.137>, 2016.

- Tomaz, S., Jaffrezo, J.-L., Favez, O., Perraudin, E., Villenave, E., and Albinet, A.: Sources and atmospheric chemistry of oxy- and nitro-PAHs in the ambient air of Grenoble (France), *Atmospheric Environment*, 161, 144–154, 935 <https://doi.org/10.1016/j.atmosenv.2017.04.042>, 2017.
- Tuet, W. Y., Chen, Y., Xu, L., Fok, S., Gao, D., Weber, R. J., and Ng, N. L.: Chemical oxidative potential of secondary organic aerosol (SOA) generated from the photooxidation of biogenic and anthropogenic volatile organic compounds, *Atmos. Chem. Phys.*, 17, 839–853, <https://doi.org/10.5194/acp-17-839-2017>, 2017.
- 940 Valavanidis, A., Fiotakis, K., and Vlachogianni, T.: Airborne Particulate Matter and Human Health: Toxicological Assessment and Importance of Size and Composition of Particles for Oxidative Damage and Carcinogenic Mechanisms, *Journal of Environmental Science and Health, Part C*, 26, 339–362, <https://doi.org/10.1080/10590500802494538>, 2008.
- Valko, M., Morris, H., and Cronin, M.: Metals, Toxicity and Oxidative Stress, *CMC*, 12, 1161–1208, <https://doi.org/10.2174/0929867053764635>, 2005.
- 945 Verma, V., Fang, T., Guo, H., King, L., Bates, J. T., Peltier, R. E., Edgerton, E., Russell, A. G., and Weber, R. J.: Reactive oxygen species associated with water-soluble PM_{2.5} in the southeastern United States: spatiotemporal trends and source apportionment, *Atmos. Chem. Phys.*, 14, 12915–12930, <https://doi.org/10.5194/acp-14-12915-2014>, 2014.
- 950 Visentin, M., Pagnoni, A., Sarti, E., and Pietrogrande, M. C.: Urban PM_{2.5} oxidative potential: Importance of chemical species and comparison of two spectrophotometric cell-free assays, *Environmental Pollution*, 219, 72–79, <https://doi.org/10.1016/j.envpol.2016.09.047>, 2016.
- Waked, A., Favez, O., Alleman, L. Y., Piot, C., Petit, J.-E., Delaunay, T., Verlinden, E., Golly, B., Besombes, J.-L., Jaffrezo, J.-L., and Leoz-Garziandia, E.: Source apportionment of PM₁₀ in a north-western Europe regional urban background site (Lens, France) using positive matrix factorization and including primary biogenic emissions, *Atmos. Chem. Phys.*, 14, 3325–3346, <https://doi.org/10.5194/acp-14-3325-2014>, 2014.
- 955 Weber, S., Uzu, G., Calas, A., Chevrier, F., Besombes, J.-L., Charron, A., Salameh, D., Ježek, I., Močnik, G., and Jaffrezo, J.-L.: An apportionment method for the oxidative potential of atmospheric particulate matter sources: application to a one-year study in Chamonix, France, *Atmos. Chem. Phys.*, 18, 9617–9629, <https://doi.org/10.5194/acp-18-9617-2018>, 2018.
- 960 Weber, S., Salameh, D., Albinet, A., Alleman, L. Y., Waked, A., Besombes, J.-L., Jacob, V., Guillaud, G., Meshbah, B., Rocq, B., Hulin, A., Dominik-Sègue, M., Chrétien, E., Jaffrezo, J.-L., and Favez, O.: Comparison of PM₁₀ Sources Profiles at 15 French Sites Using a Harmonized Constrained Positive Matrix Factorization Approach, *Atmosphere*, 10, 310, <https://doi.org/10.3390/atmos10060310>, 2019.
- Weber, S., Uzu, G., Borlaza, L. J. S., Calas, A., Salameh, D., Chevrier, F., Allard, J., Besombes, J.-L., Albinet, A., Favez, O., and Jaffrezo, J.-L.: Oxidative potential source apportionment at 15 French sites for yearly time series of observation, 2021.
- 965 Winterbottom, C. J., Shah, R. J., Patterson, K. C., Kreider, M. E., Panettieri, R. A., Rivera-Lebron, B., Miller, W. T., Litzky, L. A., Penning, T. M., Heinlen, K., Jackson, T., Localio, A. R., and Christie, J. D.: Exposure to Ambient Particulate Matter Is Associated With Accelerated Functional Decline in Idiopathic Pulmonary Fibrosis, *Chest*, 153, 1221–1228, <https://doi.org/10.1016/j.chest.2017.07.034>, 2018.
- 970 Xiong, Q., Yu, H., Wang, R., Wei, J., and Verma, V.: Rethinking Dithiothreitol-Based Particulate Matter Oxidative Potential: Measuring Dithiothreitol Consumption versus Reactive Oxygen Species Generation, *Environ. Sci. Technol.*, 51, 6507–6514, <https://doi.org/10.1021/acs.est.7b01272>, 2017.

Yang, A., Wang, M., Eeftens, M., Beelen, R., Dons, E., Leseman, D. L. A. C., Brunekreef, B., Cassee, F. R., Janssen, N. A. H., and Hoek, G.: Spatial Variation and Land Use Regression Modeling of the Oxidative Potential of Fine Particles, *Environmental Health Perspectives*, 123, 1187–1192, <https://doi.org/10.1289/ehp.1408916>, 2015.

975 Yu, H., Wei, J., Cheng, Y., Subedi, K., and Verma, V.: Synergistic and Antagonistic Interactions among the Particulate Matter Components in Generating Reactive Oxygen Species Based on the Dithiothreitol Assay, *Environ. Sci. Technol.*, 52, 2261–2270, <https://doi.org/10.1021/acs.est.7b04261>, 2018.

Yu, S., Liu, W., Xu, Y., Yi, K., Zhou, M., Tao, S., and Liu, W.: Characteristics and oxidative potential of atmospheric PM_{2.5} in Beijing: Source apportionment and seasonal variation, *Science of The Total Environment*, 650, 277–287, <https://doi.org/10.1016/j.scitotenv.2018.09.021>, 2019.

980 Zhou, J., Elser, M., Huang, R.-J., Krapf, M., Fröhlich, R., Bhattu, D., Stefenelli, G., Zotter, P., Bruns, E. A., Pieber, S. M., Ni, H., Wang, Q., Wang, Y., Zhou, Y., Chen, C., Xiao, M., Slowik, J. G., Brown, S., Cassagnes, L.-E., Daellenbach, K. R., Nussbaumer, T., Geiser, M., Prévôt, A. S. H., El-Haddad, I., Cao, J., Baltensperger, U., and Dommen, J.: Predominance of secondary organic aerosol to particle-bound reactive oxygen species activity in fine ambient aerosol, *Atmos. Chem. Phys.*, 19, 14703–14720, <https://doi.org/10.5194/acp-19-14703-2019>, 2019.

985